SWARTHMORE COLLEGE DEPARTMENT OF ENGINEERING

SIMULTANEOUS LEVITATION & POWER BY INDUCTION

RICHARD METZLER '06

SENIOR DESIGN THESIS: FINAL REPORT
ADVISOR: ERIK CHEEVER
SUBMITTED MAY 4, 2006

SWARTHMORE COLLEGE
INCORPORATED 1864

E90: FINAL REPORT

SIMULTANEOUS LEVITATION & POWER BY INDUCTION

TABLE OF CONTENTS

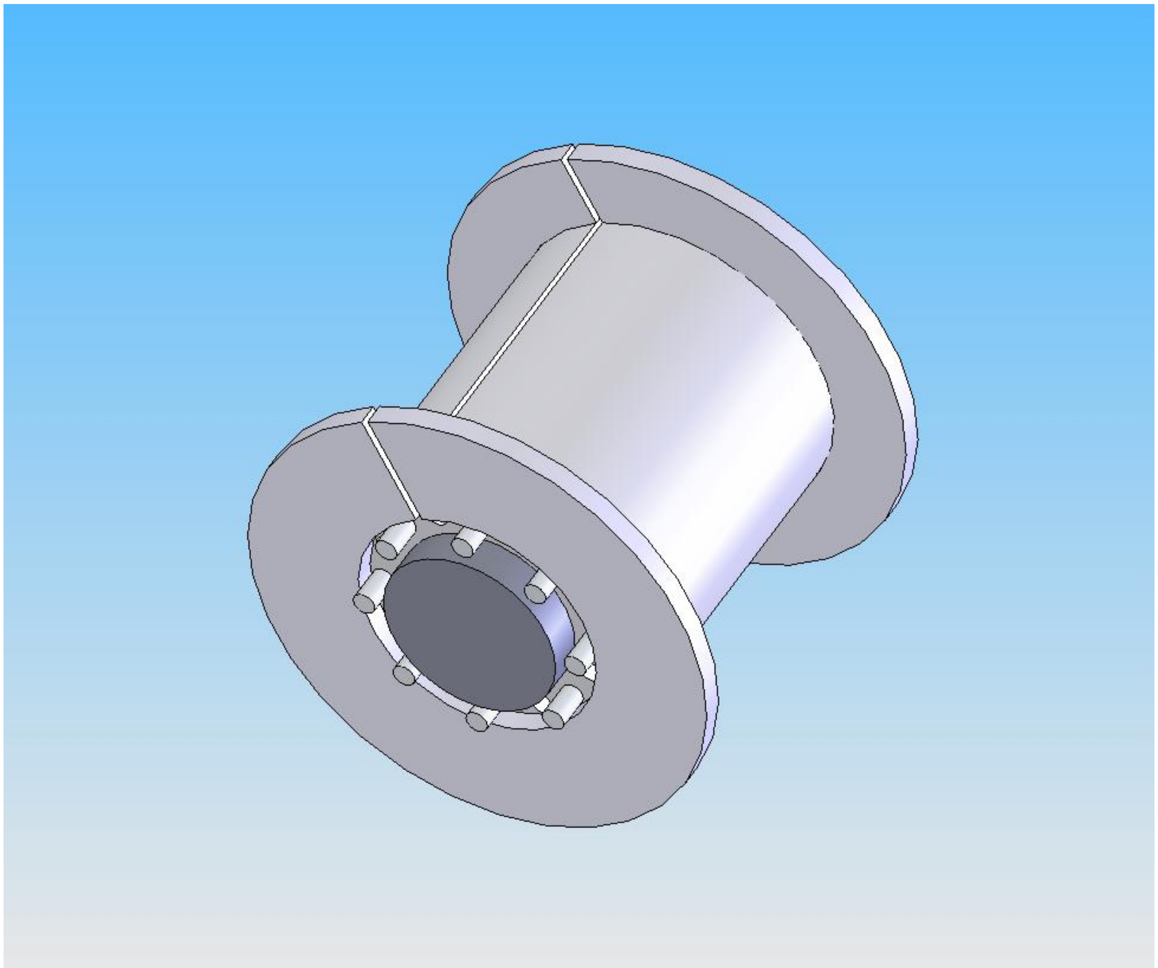

Figure 1: Levitation System

ABSTRACT

The goal of this project is to simultaneously levitate and power an autonomous device in a controlled manner. The system of particular interest—a conductive ring, driven by a solenoid—could be used to power machinery mounted on the ring without the means of an onboard power supply. This induced power is supplied by the stored momentum of the magnetic field generated by the solenoid when the field is altered. The induced current in the ring is be rectified and used to run electrical components on the ring itself, without the added weight of a battery. Thus, the design of this control unit could lead to the eventual design of a circuit that can run automatically from induced power, and could be controlled to move in three dimensions by adjustment of feedback controlled electromagnets.

INTRODUCTION

Applications for an autonomous levitation system range from design of small sensor devices to explore tight spaces such as vertical pipes or ducts where defects must be mapped, to uses as discrete surveillance systems. Expansion of the idea to a three-dimensional control system could be advantageous to applications requiring minimal friction and as in bearings or transport systems. Indeed, current magnetic levitation train technologies rely on three expensive methods of levitation and propulsion which could be somewhat curbed by more efficient use of energy. EDS (*Electrodynamic Suspension*)-type Mag-Lev's rely on superconducting materials which require constant cooling by heavy, expensive liquid helium refrigeration systems in order to maintain perfect conductivity. Permanent magnet systems such as the *Inductrack* rely on a passive magnetic field but can only achieve levitation at high speeds. These systems must also use an external propulsion system to move and guide the train. EMS (*Electromagnetic Suspension*) trains are the in most widespread use and rely on feedback controlled electromagnets to both levitate and propel the train. These require high currents but have the advantage of supplying continuous levitation and providing propulsion. Simultaneous power by induction could allow for more efficient use of the energy required to run this type of train allowing onboard electronics formerly run by heavy auxiliary battery systems to use the power typically lost during the levitation process.

Difficulties arise in control of such a system due to the intrinsic nonlinearity of the repulsive force with respect to supplied current, and the nonlinear relation to the induced current and position of the suspended device. The latter case can easily be accommodated to supply an onboard chip with power through use of zener diode (within a certain tolerance of position). Position control can be accomplished by feeding back the intensity of an IR LED or radio antenna powered on the suspended loop (included in the LOAD in the figure to the right) to a sensor driven state estimator connected to the electromagnet. The equations of motion relating the levitation force to the input to the magnet can be linearized about an equilibrium point and the appropriate state estimator implemented.

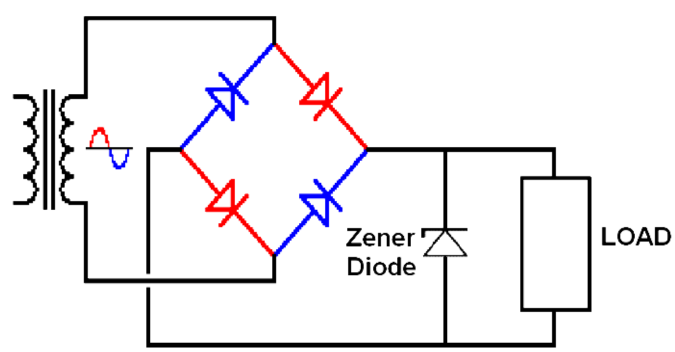

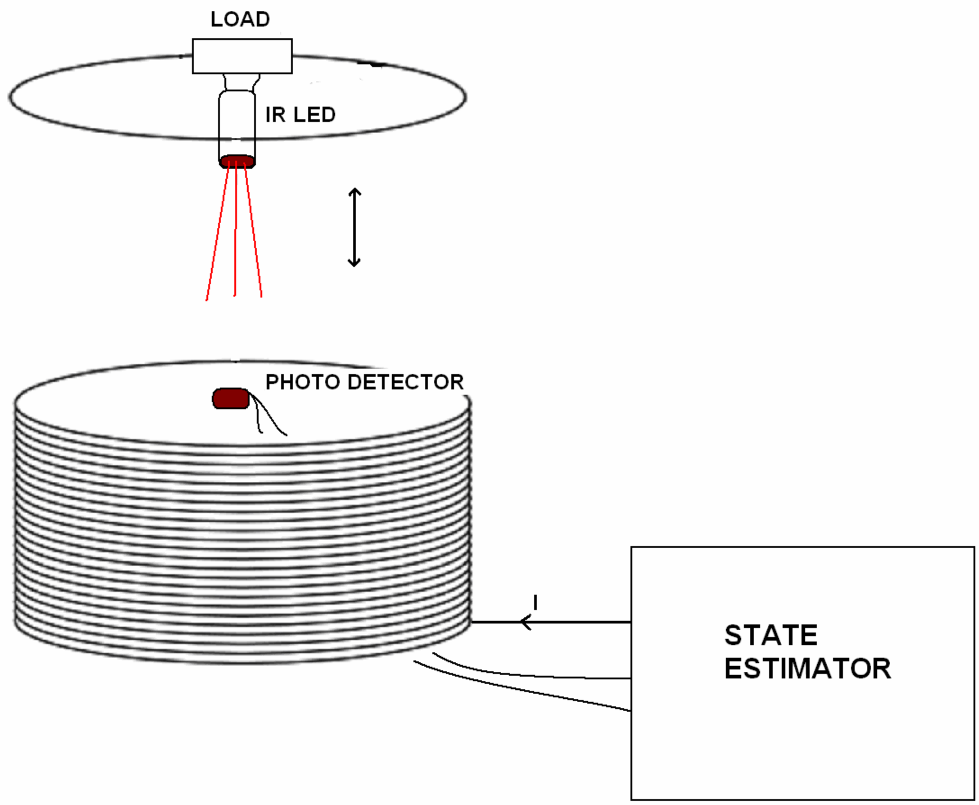

Figure 2: Photoelectric Position Feedback System in Proposed Levitation Device.

DESIGN

I. SOLENOID DESIGN:

INITIAL CRITERIA

Originally, a conductive coil was to be levitated above the power solenoid by the Lorentz force law. This repulsive force is proportional to the time derivative of the supplied magnetic field from the power solenoid. Thus, if the solenoid is powered by a sinusoidal voltage, the force is proportional to the amplitude A times the natural frequency ω. A simple model for the power solenoid is given by the RLC circuit shown below

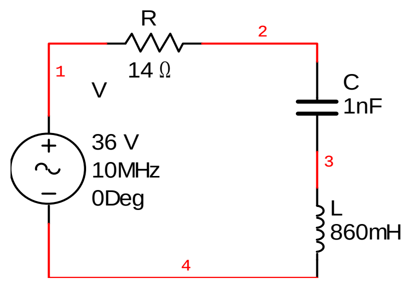

Figure 3: 2nd Order Solenoid Model

with the generated field proportional to the current. To maximize the repulsive force without requiring significant power consumption, the solenoid would be wound such that its resonant frequency would be about 10 MHz.

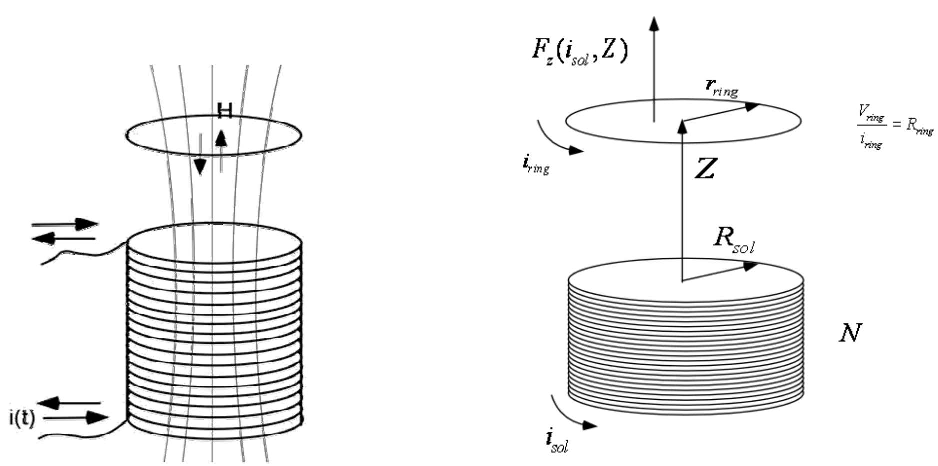

Figure 4: The system. A current $i(t)$ is driven through the solenoid. This current will produce a force F_z on the ring that is proportional to the current and to the height Z of the ring itself.

We begin by defining the force on the ring by using the Lorentz Force Law, which states that the repulsive force on a unit with a current *I* due to a magnetic field $\vec{B}$ is given by:

$$\vec{F} = \oint I\left(dl \times \vec{B}\right) \tag{1}$$

The total force on the ring will then be the integral of the Lorentz law (1), applied to some differential length dl in the ring. We know from symmetry that the net force must be in the $\hat{z}$ direction: all other components will cancel out when we take the integral around the loop. From (1) above we get:

$$F_z = \oint dl \cdot I_{\hat{\theta}} \cdot B_r \tag{2}$$

where we have taken the scalar components of the vector quantities $\vec{B}$ and $I_{\hat{\theta}}$ as we are only interested in one component of each (we set $B = B_{\hat{r}}$ and $I = I_{\hat{\theta}}$). We find that the current and the magnetic component are symmetric around the loop, so the integral is becomes trivial, and we get:

$$F_z = 2\pi r \cdot I_{ring} \cdot B_r \tag{3}$$

Now, we can use the geometry of the system to find B_r. We take as a control volume a cylinder the size of the ring, with radius r, and some differential height dz:

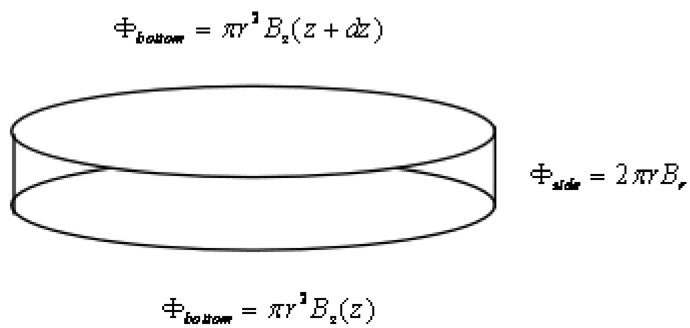

Figure 5: The flux diagram for the cylindrical control volume. We see that the total flux must be equal to zero, so the flux lost through the sides must be the net flux gained through the top and bottom.

We must have a total flux equal to zero in our control volume, since it only contains empty space. We know we gain some flux through the bottom, lose some through the top, and also lose some through the sides. We have expressed these values above as a product of the magnetic flux density and the surface area. By setting the total flux equal to zero to satisfy this continuity condition, we get:

$$0 = 2\pi r B_r - \pi r^2 \frac{\partial \vec{B}}{\partial z} \tag{4.a}$$

which simplifies to:

$$B_r = \frac{-r}{2}\frac{dB_z}{dz} \tag{4.b}$$

Then,

$$F_z = -\pi r^2 \cdot I_{ring} \cdot \frac{dB}{dz} = -\pi r^2 \cdot \frac{dB}{dz} \cdot \frac{V_{ring}}{R_{ring}} \tag{5}$$

where

$$B(z,i) = \frac{\mu_o N i}{2} \frac{R^2}{\left(R^2 + z^2\right)^{3/2}} \tag{6}$$

and V_{ring} is the induced EMF in the ring, which is given by Faraday's Law:[1]

$$\begin{aligned} V_{\mathrm{EMF}} &= -\frac{d\Phi}{dt} = -A \cdot \frac{dB_z}{dt} \\ &= -\pi r^2 \mu_0 N \frac{R_{sol}{}^2}{\left(R_{sol}{}^2 + Z(t)^2\right)^{3/2}} \cdot \frac{di_{sol}(t)}{dt} \end{aligned} \tag{6.a}$$

Here N is the number density of windings in the solenoid, and we have assume that Z*(t)* does not change appreciably in time. Thus, the simple result for the induced voltage is

[1] Griffiths

$$V_{\text{EMF}} = -\frac{K}{\left(R_{sol}{}^2 + Z(t)^2\right)^{3/2}} \cdot \frac{di_{sol}(t-\theta)}{dt} \tag{6.b}$$

where K is a constant lumping up the messy system parameters and theta is some phase lag owing to the self inductance of the ring (we will return to this later).

We also need an expression for $\frac{dB_z}{dz}$, for which we get[2]:

$$\frac{dB_z}{dz} = \frac{\partial}{\partial z}\left[\frac{\mu_0 i_{sol}(t) N}{2} \frac{R_{sol}{}^2}{\left(R_{sol}{}^2 + Z(t)^2\right)^{3/2}}\right] = -\frac{C \cdot Z(t) \cdot i_{sol}(t)}{\left(R_{sol}{}^2 + Z(t)^2\right)^{5/2}} \tag{7}$$

where we have again grouped constants into C for brevity. Plugging (6) and (7) back into (5), we get:

$$\begin{aligned} F_z &= \frac{2\pi}{R_{ring}} \frac{K}{\left(R_{sol}{}^2 + Z^2\right)^{-3/2}} \frac{C \cdot Z(t)}{\left(R_{sol}{}^2 + Z(t)^2\right)^{5/2}} i_{sol}(t) \cdot i'_{sol}(t-\theta) \\ &= D \frac{Z(t) \cdot i_{sol}(t) \cdot i'_{sol}(t-\theta)}{\left(R_{sol}{}^2 + Z(t)^2\right)} \\ &\approx \frac{D \cdot i_{sol}(t) \cdot i'_{sol}(t-\theta)}{Z(t)} \end{aligned} \tag{8}$$

where we have assumed in the last approximation that the distance *Z(t)* above the solenoid is much larger than the radius of the solenoid itself.

We can now find the equations of motion by using Newton's First Law ($F = m\ddot{Z}(t)$). We assume that the only forces acting on the system are gravity and the Lorentz Force, so we wind up getting:

$$m\ddot{Z} = \frac{D \cdot i(t) \cdot i'(t-\theta)}{Z} - mg \tag{9.a}$$

Or

[2] Griffiths

$$\ddot{z} = \frac{D}{m}\frac{i(t)\cdot i'(t-\theta)}{Z} - g \tag{9.b}$$

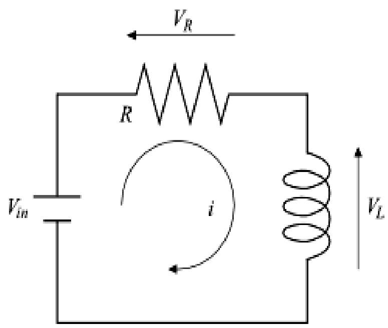

The derivative term can be misleading in that the force is not generated by the current of the solenoid; rather, it is generated by the opposing magnetic fields of the ring and the solenoid (which has an *i(t)* dependence) and the ring (which is dependent on the derivative of *i(t)*). The phase lag θ is included here to indicate that the opposing magnetic field of the ring is not necessarily instantaneously induced by the oscillating magnetic field of the solenoid. In fact the ring itself is an inductor and will introduce this phase lag between the generated current and the induced EMF generated by the solenoid current. If the capacitance of the between the coils is negligible, we can use a simple RL circuit to model this. Notice that the average force is zero unless the field generating current, i_{sol}, is in phase with the induced current's derivative.[3] We can use the self-impedance relationship for the ring to find the phase lag of induced current's derivative in terms of the EMF voltage generated by i_{sol}.[4]

$$i'_{sol}\left(t-\theta\right) = i'_{ring}\left(t\right) = \frac{1}{L}\left(V_{\mathrm{EMF}}\left(t\right) - R\cdot i_{ring}\left(t\right)\right) \tag{10}$$

where R is the resistance of the ring and L is its self-inductance. Taking the Laplace Transform and solving for the transfer function of the derivative we get:

$$T(s) = \frac{1}{R}\cdot\frac{s}{\left(\frac{L}{R}s+1\right)} \tag{11}$$

We get the following Bode plot:

[3] Notice that for any periodic waveform such as a sinusoid, the derivative is 90° out of phase. Thus the average of the signal times its derivative must be an odd function with average zero.
[4] Purcell

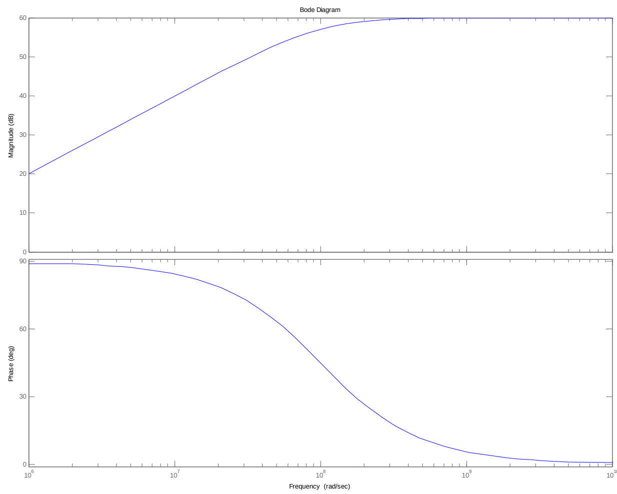

Figure 6: Bode Plot of Current through Levitation Ring

where we can see that the phase only approaches zero when the circuit is driven an order of magnitude greater than the pole frequency L/R where it also approaches its maximum gain. Thus, experimentally it appears that the induced force is proportional to the square of the amplitude of the supplied solenoid current over the height of flotation for high driving frequencies with respect to L/R.:

$$\boxed{\ddot{z} \approx k\frac{i^2(t)}{mZ} - g} \tag{9.c}$$

MATERIALS SELECTION

In constructing the power solenoid, special care was taken to use the proper materials to produce the maximum field strength that could be oscillated megahertz frequencies. Here I will discuss some of the concepts involved in materials selection of suitable magnetic materials.

Magnetic fields in matter are rated by the *magnetic flux density* (or *magnetic induction*) *B*. This quantity gives measure to the quantity magnetic field lines passing through a surface per unit area and is proportional to the ambient *magnetic field strength H* plus the *magnetization M* of the medium by the *permeability of free space* μ_o:

$$B = \mu_o\left(H + M\right), \tag{10}$$

where $\mu_o = 4\pi \times 10^{-7}$ N/A^2. In general, the magnetization itself is proportional to the magnetic field strength by the linear magnetic susceptibility χ_m. Then,

$$
\begin{aligned}
B &= \mu_o \left(1 + \chi_m\right) H \\
&= \mu H
\end{aligned}
\tag{11}
$$

where μ is the medium's *magnetic permeability*. Often however, materials are characterized by their *relative permeability*

$$
\mu_r = \frac{\mu}{\mu_o}\,. \tag{12}
$$

In order to support and enhance the magnetic field strength H supplied by a current-carrying coil, high permeability ferromagnetic materials should be used for a solenoid's core.

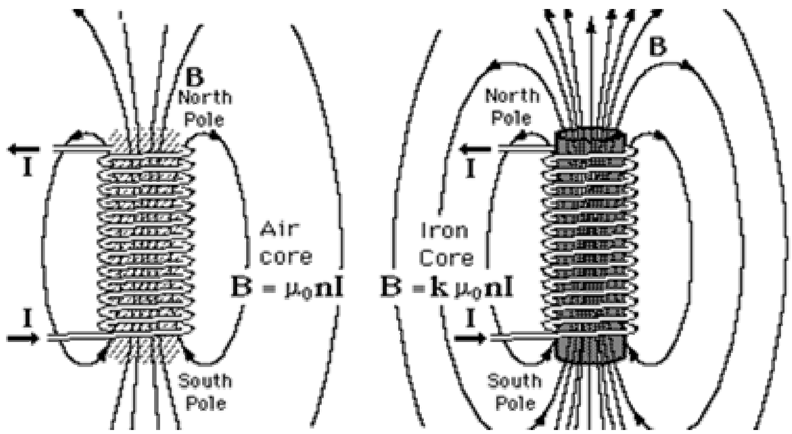

[5]

Figure 7: Magnetic Fields trough Vacuum and through Iron

One must also consider that the saturation flux density of any given material will limit its maximal performance; that is, once the magnitude of the field strength reaches a certain value, all magnetic dipoles will be aligned with the field and further magnetization cannot take place. Typically, iron has a saturation flux density of about 2 T. This is an upper value in typical NMR machines. In cores which must support magnetic fields greater than this such as in an MRI which requires flux densities of 40 T, air can be used as the core material as it will not saturate. However, because air has a relative permeability of only 1, one would need to provide 150 times more field strength than necessary to generate the same flux density within an iron core with a typical relative permeability of 150.

Another important factor is hysteresis loss. The graph below shows the B field as a function of the H field.

[5] http://hyperphysics.phy-astr.gsu.edu/hbase/magnetic/elemag.html#c4

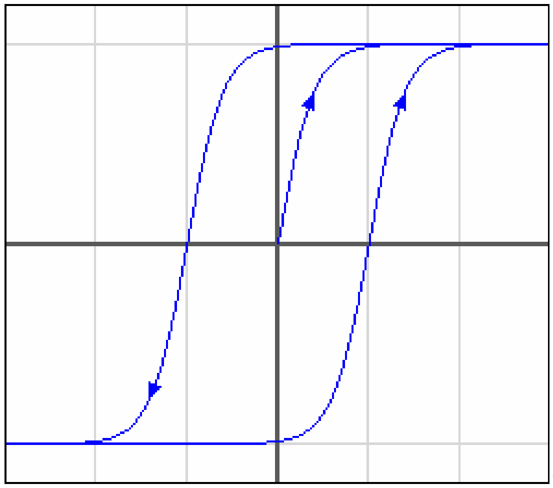

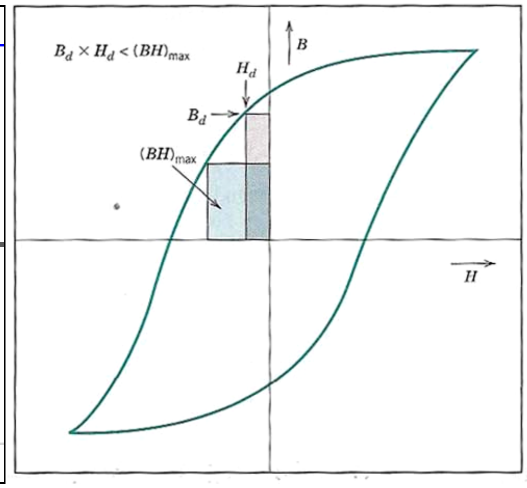

Figure 7
Figure 8: B vs H of a typical ferromagnetic material.

Note that the magnetic flux density is path dependent. In traversing the curve, the area enclosed by the path is the energy cost of changing the magnetization of a material. This is usually released as thermal energy at the expense of the induced field in a solenoid core. The saturation flux density can also be determined from the curve and is given by magnitude at the cusps of the hysteresis curve where the magnitude of B approaches the horizontal asymptote. The permeability of the material is given by the slope of the curve at any given point and is seen to be dependent on H. The initial permeability is that given on most data tables and is the slope of the path starting from the origin. Here is good place to elucidate the meaning of permeability: It is a measure of how easy/difficult it is to rotate the magnetic dipoles within a medium.

Materials that have a narrow hysteresis curve experience little energy loss in the presence of a changing H field and are dubbed "soft" magnetic materials. These usually have steep curves originating from the origin and thus have very high initial permeabilities. "Hard" magnetic materials on the other hand undergo massive core loss and require massive amounts of energy to change their magnetization. For this reason, hard magnetic materials have a large *remenancy*; that is, they generally hold their magnetization indefinitely unless forcefully altered.

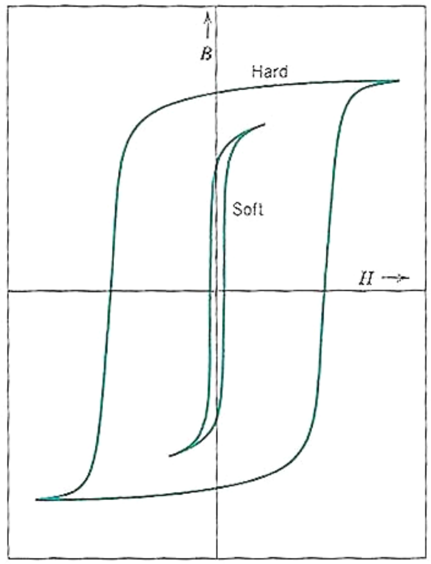

6

Figure 9: Hysteresis Curves of Hard and Soft Magnetic Materials

For these reasons, soft magnetic materials are preferred for AC operation. A table of soft magnetic materials is given below and a chart of hard magnetic materials in the following section.

Table 1: Table of Soft Magnetic Materials

Material	*Composition* (*wt %*)	*Initial Relative Permeability* μ_i	*Saturation Flux Density* B_s [*tesla* (*gauss*)]	*Hysteresis Loss/Cycle* [J/m^3 (erg/cm^3)]	*Resistivity* ρ (Ω-*m*)
Commercial iron ingot	99.95Fe	150	2.14 (21,400)	270 (2700)	1.0×10^{-7}
Silicon–iron (oriented)	97Fe, 3Si	1400	2.01 (20,100)	40 (400)	4.7×10^{-7}
45 Permalloy	55Fe, 45Ni	2500	1.60 (16,000)	120 (1200)	4.5×10^{-7}
Supermalloy	79Ni, 15Fe, 5Mo, 0.5Mn	75,000	0.80 (8000)	—	6.0×10^{-7}
Ferroxcube A	$48MnFe_2O_4$, $52ZnFe_2O_4$	1400	0.33 (3300)	~40 (~400)	2000
Ferroxcube B	$36NiFe_2O_4$, $64ZnFe_2O_4$	650	0.36 (3600)	~35 (~350)	10^7

[6] Callister, 690

Table 2: Soft Magnetic Materials Listing from Ed Fagan Inc.[7]

Typical DC Magnetic Properties					
	EFI 79	EFI 50	EFI Co50	EFI Core Iron	EFI Vac Iron
Saturation Induction - Gauss	8,700	14,500	24,200	21,500	21,500
Maximum Permeability	230,000	100,000	10,000	10,000	10,0000
Coercive Force - Oersteds	0.015	0.060	0.400	1.000	1.000
amps per m	1.19	4.77	31.83	79.58	79.58
Typical AC Magnetic Properties					
Core Loss W/lb @400Hz & 20k G	N/A	N/A	34	N/A	N/A
B-40 Permeabilty @60Hz	45,000	6,500	N/A	N/A	N/A
NA = Not reported, not a typical application value					

One other consideration is important to take into account: resistance. An oscillating magnetic field induces an electromotive force which causes current to flow in the opposite sense to the current supplied through the coil. This manifests in magnetization opposite the desired direction and effectively increases the impedance of the coil. This mutual inductance is exactly what we want in the floatation coil but is a hindrance to the performance of the solenoid of the solenoid. Because of this we require a core material with very high resistance which will keep eddy currents to a minimum. Other tricks can be employed to lessen eddy currents such as eliminating any circular paths for current to flow or by using laminations to prevent current flow from one sheet to the next.

CONSTRUCTION & MODIFICATION

Noting that an alternating magnetic field will also induce a back EMF into the winding itself thereby impeding the flow of current, effort was taken to minimize the self-inductance

$$L \propto \mu_o \frac{n^2}{l} \tag{13}$$

The strength of the field depends on n so it is not desirable to minimize this quantity too much, rather, by maximizing the length of the solenoid l we can minimize the self-inductance affordably.

A 7" long, 4" inner diameter steel spool was to be constructed for winding the coil. To maximize the saturation density, EFI Co50 alloy rods were held in a primarily air core by insulative phenolic sleeves which were pressed into the spool which was to be wound with the proper magnet wire.

[7] www.edfagan.com

The proper solenoid winding gauge was determined by an appropriate java script (see APPENDIX) by comparing the winding density (a positive factor in contribution to the net magnetic field) to the net impedance of the solenoid for each gauge. Also considering price constraints and availability, 30 lbs (almost one mile) of AWG 16 gauge magnetic wire rated at 300° C was chosen. The core was wound from 4.3" to 6.9" in diameter (about 21 layers of winding) and had a DC impedance of about 14 Ohms. Winding was done originally to be done on a lathe, but even on the lowest speed setting, windings would jump and slide creating air gaps which decrease the winding density. This was also intolerable because thermal expansion and strain working of the wires during AC operation would cause windings to rub insulation off and short together whole layers. For these reasons, winding of the solenoid was done painstakingly by hand.

In order to reduce the total impedance of the core, it was initially planned to wire every two layers of wiring in parallel with the next two successive layers.

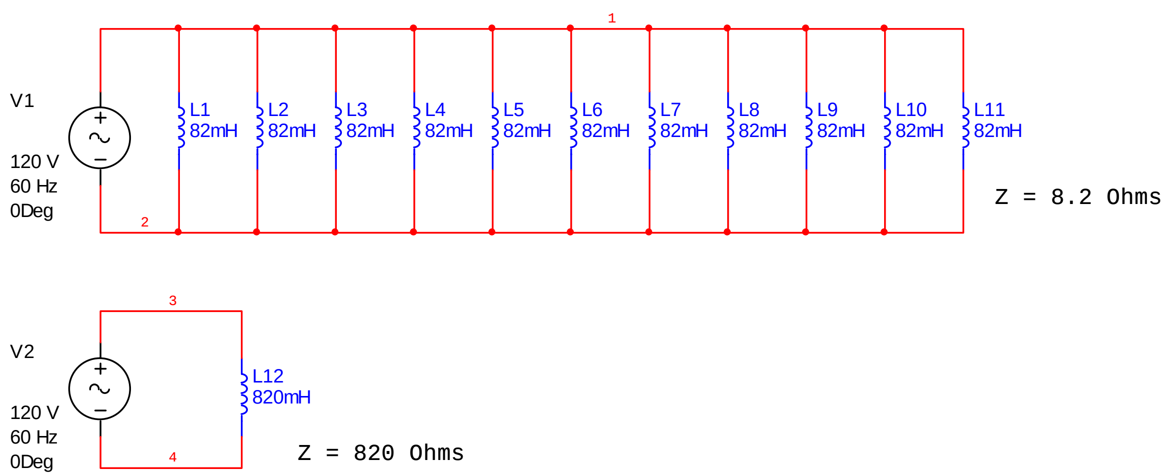

Figure 10: Dividing Inductance for Solenoid Winding

This reduces the necessary driving voltage to below the safe limit of 48 V but requires a significant amount of amperage. Because the power supplies available for use could only deliver a total of 5.6 A, a continuously wound magnet was built instead, with a maximum possible voltage drop of 70 V to accommodate the limitation. Because a series aligned inductances add while a parallel alignment diminish, the total impedance was sacrificed for current performance, which is the contributor to the magnetic field. However, the power supplies were only able to deliver up to 20 kHz AC current without significant attenuation, limiting the electromagnet's response orders of magnitude below the ten megahertz resonant frequency.

Inductive power supplied to the solenoid at 5 A amplitude, 20 kHz frequency was insufficient to jump a 7" ID, 8" OD ring without extending the solenoid core through the center of the ring. Because the levitating device was to be completely free-floating, this was an unacceptable condition.

To compromise for the lack of repulsive force, the entire system was flipped upside-down and the solenoid was fitted with a 3" diameter, one inch thick, high power N48 neodymium magnet.

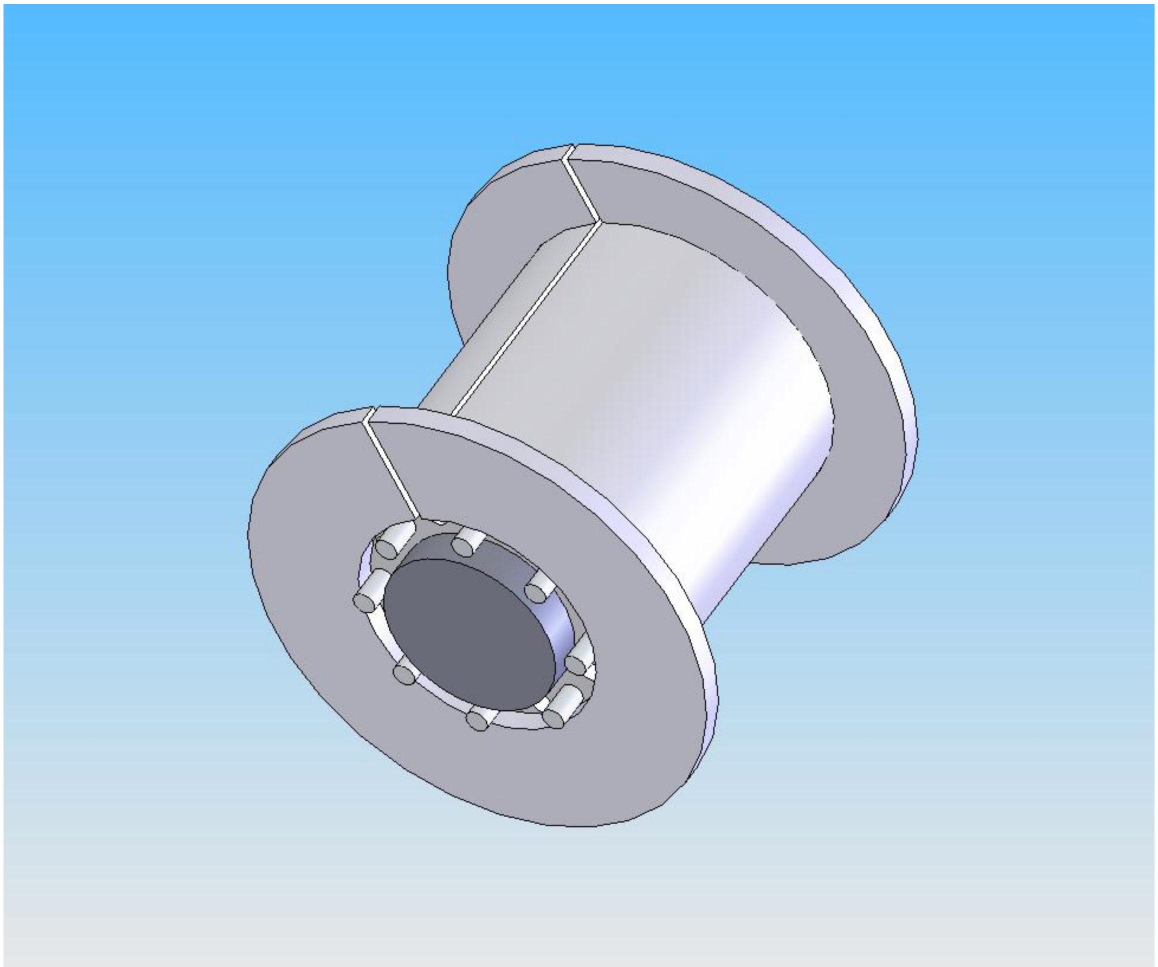

Figure 11: Solenoid with Permanent Magnet

At the time, N48 was the highest grade magnet available in size. Several weeks later higher grades N50 and N52 advertising higher flux densities came on the market.

The magnet alone allows astable floatation of a one inch diameter by one inch thick N50 neodymium magnet up to 8 inches. However, because a hard magnetic material is now introduced to the core (already near saturation) further boosting of the auxiliary field produced by the coil is limited.

Table 3: Table of Hard Magnetic Materials

Material	*Composition* (*wt %*)	*Remanence* B_r [*tesla* (*gauss*)]	*Coercivity* H_c [*amp-turn/m* (*Oe*)]	$(BH)_{max}$ [kJ/m^3 (*MGOe*)]	*Curie Temperature* T_c [°*C* (°*F*)]	*Resistivity* ρ (Ω-*m*)
Tungsten steel	92.8 Fe, 6 W, 0.5 Cr, 0.7 C	0.95 (9500)	5900 (74)	2.6 (0.33)	760 (1400)	3.0×10^{-7}
Cunife	20 Fe, 20 Ni, 60 Cu	0.54 (5400)	44,000 (550)	12 (1.5)	410 (770)	1.8×10^{-7}
Sintered alnico 8	34 Fe, 7 Al, 15 Ni, 35 Co, 4 Cu, 5 Ti	0.76 (7600)	125,000 (1550)	36 (4.5)	860 (1580)	—
Sintered ferrite 3	$BaO\text{–}6Fe_2O_3$	0.32 (3200)	240,000 (3000)	20 (2.5)	450 (840)	$\sim 10^4$
Cobalt rare earth 1	$SmCo_5$	0.92 (9200)	720,000 (9,000)	170 (21)	725 (1340)	5.0×10^{-7}
Sintered neodymium-iron-boron	$Nd_2Fe_{14}B$	1.16 (11,600)	848,000 (10,600)	255 (32)	310 (590)	1.6×10^{-6}

[8]

In this scheme, it is necessary to "drop" a floating magnetic object by enhancing or attenuating the supplied **DC** current to the electromagnet rather than propelling a conductive ring with **AC** current. The AC component to power a coil mounted on the floatation magnet will also influence the total attraction and be the manifestation of the supplied inductive power.

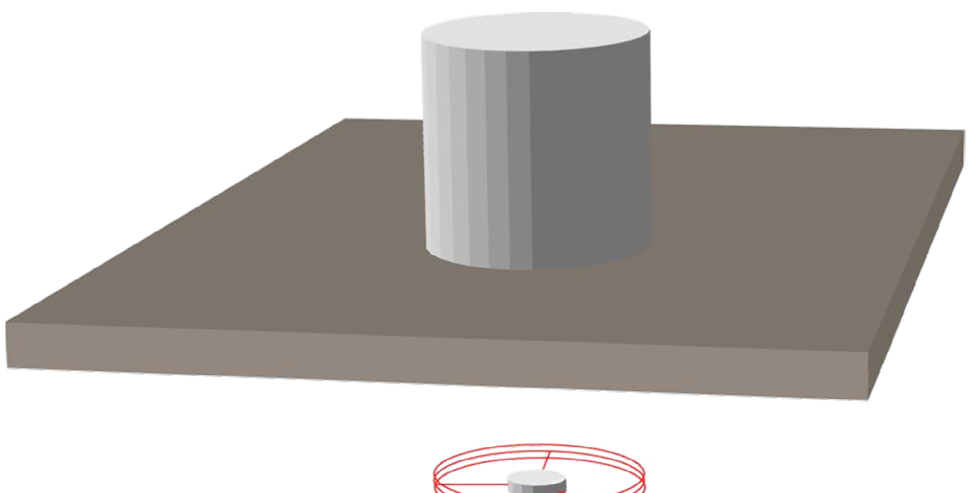

Figure 123: Magnetic Suspension

[8] Callister, 693

The force between two magnetic fields is proportional to the net flux between the generators of those fields. In thus case a solenoid, a large permanent magnet, and a floating permanent magnet contribute the total flux. Geometrically, the magnet field of a cylindrical magnet and the magnetic field of a current carrying coil of wire are indistinguishable. Thus, the total force on the floating magnet will be proportional to its static B-field times that of the solenoid plus its B-field time that of the permanent magnet. Considering Equation (6), the force becomes approximately

$$F(z,i) = \frac{m_1 i}{\left(z - m_2\right)^{9/4}} + \frac{m_3}{\left(z - m_4\right)^{9/4}} \tag{14}$$

The m_i's are fit parameters grouping all the geometrical factors found in the similar derivation of the inductive force. m_1 and m_3 scale the strength of the solenoid and the permanent magnet, respectively, while m_2 and m_4 account for the effective distances from the solenoid to the floating magnet and from the permanent magnet to the floating magnet (with contributions from their radii).

POWER SUPPLY REVISITED

Noting that the induced voltage to the levitation coil is proportional to both the frequency and magnitude of the current in the solenoid wining,

$$\left|V_{EMF}(t)\right| \propto -\mu_o n f \left|i(t)\right|, \tag{15}$$

one option to improve power performance is to exchange driving frequency for amplitude. This may be accomplished by driving the solenoid at 60 Hz (near its DC impedance) with substantial current drawn from the AC outlet. On average, the net DC force on the levitating magnet would be zero; however, this current could be rectified to produce an only positive or negative-sensed current to supply the appropriate magnetic field.

A better idea is to rectify both positive and negative components of a wall outlet's voltage to supply DC power to a fast push-pull amplifier.

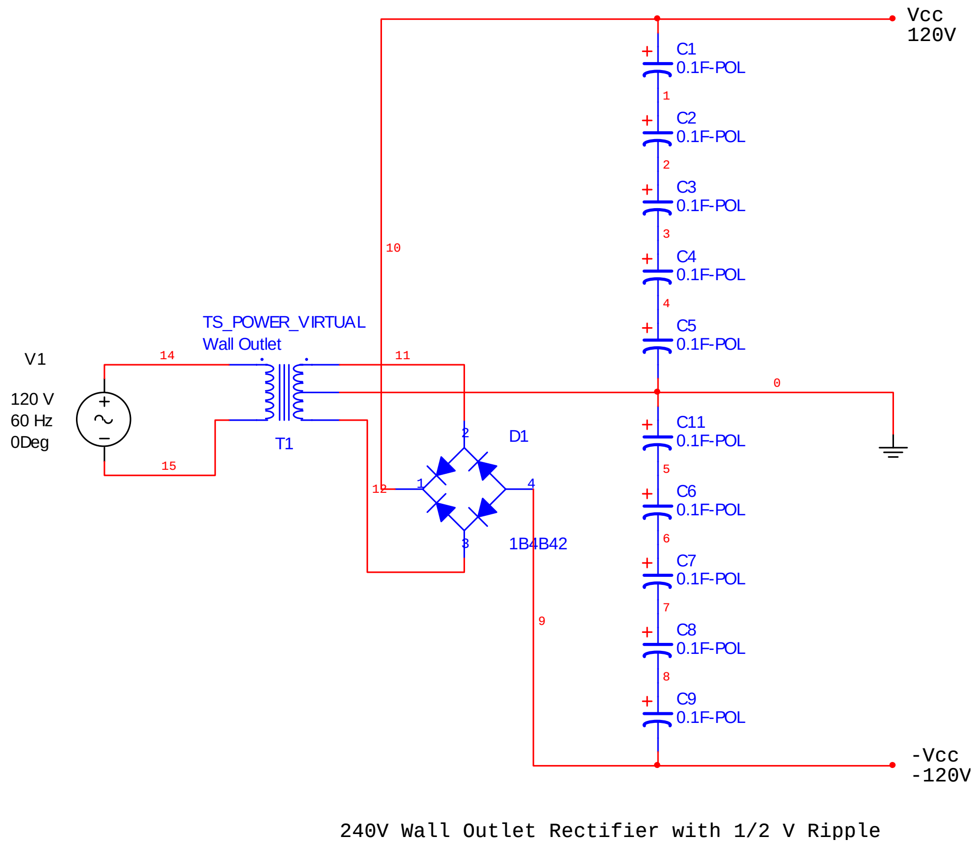

Figure 13: Rectifying Power from the Wall Outlet

The positive component is taken and smoothed by five 100,00uF capacitors rated at 25V each to minimize ripple to ½ V (0.42%). The same is done on the negative side of the circuit. The outputs are then connected to the terminals of a two stage push-pull amplifier.

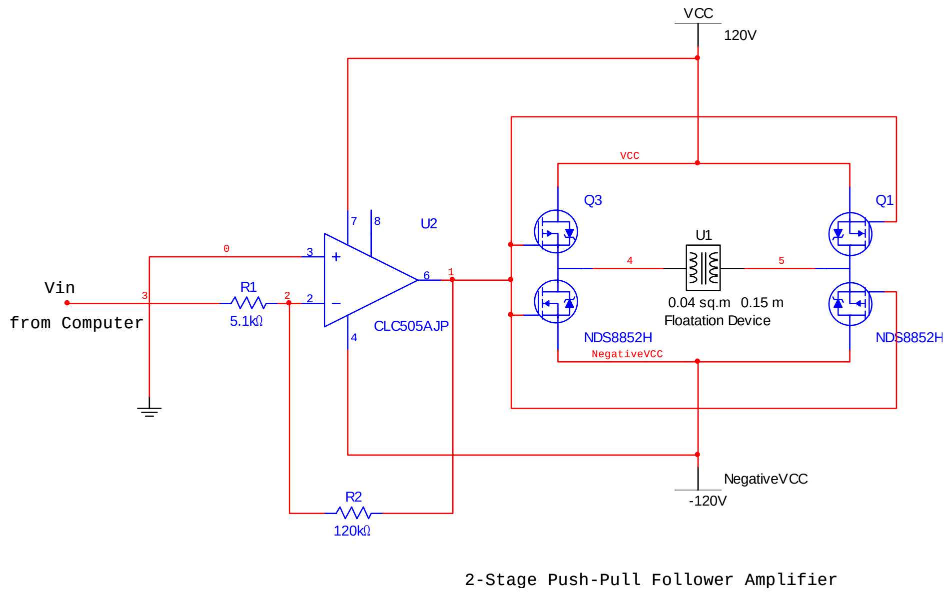

Figure 14: Push-Pull Amplifier

The amplifier follows a -5 to 5V output signal from the computer and is limited in speed by the op-amp (the transistors in use here are relatively fast). The output of the controller can be effectively amplified to up to 240V as the first stage of the amplifier pulls one terminal of the load up to +120V while the second stage pulls the other terminal down to -120 V (and vise-versa).

If faster switching speeds are required for induction, a comparator with a PWM input signal from the computer could be used instead of the op-amp. This would not be difficult to realize implement; however, because of time constraints, converting the output from the controller to a PWM signal was never implemented.

II. Position Sensing:

Theory

To complete the feedback loop it is necessary to know something about the state of the levitating object. This can be accomplished by position sensing. There are several methods of doing this:

- Hall Effect Sensing
  - One Hall Sensor is placed in a location where it can only measure the B field of the solenoid.

- Another is placed in a location where it measures the total field from the solenoid and the floatation magnet.
- Based on the difference between the signals the position of he floating magnet can be determined.
- This method can be unreliable and is subject to interference.

- Optical Interference
  - The beat pattern between a laser beam and its reflection of the floating object is measured to determine distance.

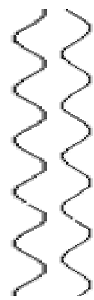

  - This requires complex and expensive equipment.
  - While this offers the best resolution of any method, it is only good over a short distance.

- Triangulation
  - Light is sent at an angle to the object and the reflection's position is measured

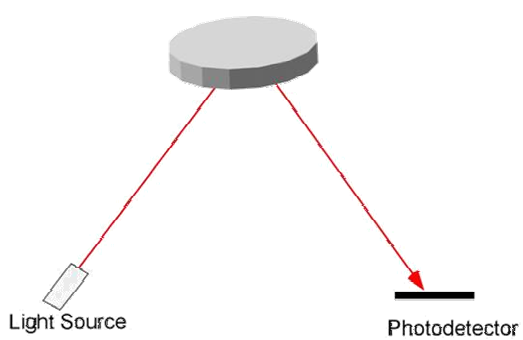

  - While the equipment isn't limitingly expensive, the long photodetector needed to measure displacements can cost well over $60.00.
  - Alignment is difficult.

- Time Of Flight
  - Easy to implement.

- Requires fast electronics for nanosecond measurements.
- Accurate measurement.

- Optical Intensity
  - Easy to implement.
  - Requires filtering which limits speed of acquisition.
  - Reasonably accurate measurement.

Although I considered using triangulation, the last two methods appeared to be better at providing distance data over long distances. I will go into more detail on these methods below.

For the time of flight method, laser light is be pulsed and the time it takes to return to a photodiode receiver will provide two times the distance to the object off which the pulse is reflected:

$$d = \frac{ct}{2} \tag{16}$$

Similar measurements can also be achieved using ultrasound.

For a cost effective solution, the magnitude of a certain wavelength of light reflected from the object of interest can be measured. This is the optical intensity method. In this case, an IR LED is flashed at 20 kHz and is received by a photodiode. The photodiode's output is digitally filtered to produce only the clocked Fourier spectrum and the magnitude measured to determine the distance regardless of ambient conditions. The output must be calibrated against the known position (leading to inaccuracies) and the method is also relatively slow. For these two reasons, modern control techniques cannot be used as accurate derivative (velocity) feedback cannot be obtained. An example output from the system is shown below:

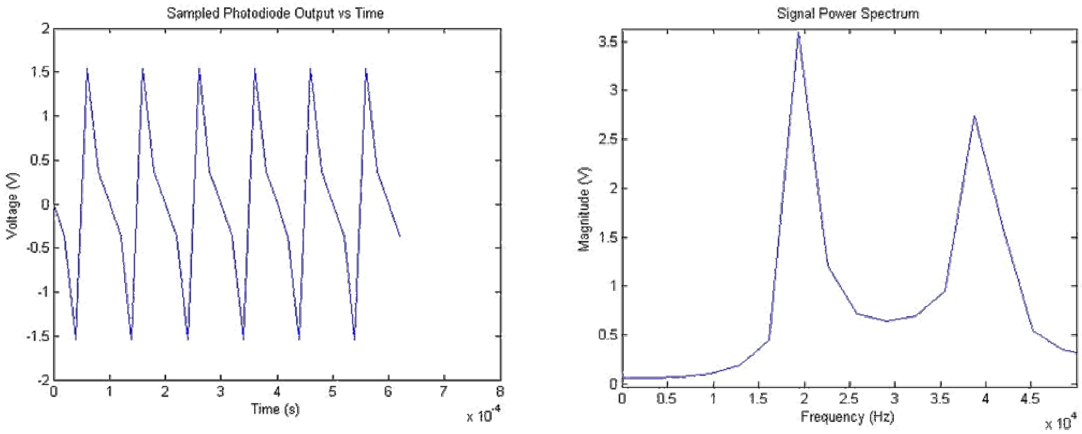

Figure 16: Position Detector Signal Output (in Volts)

For better accuracy and speed an IR laser could be used instead of the LEDs. Although IR laser diodes are readily available for about $20, pulsed versions require a relatively large supply current (typically 1.4 to 12A). Without stringing together a row of smaller power supplies to provide the necessary current, it was not possible to attain such a current with the equipment available to us (the large power supplies were already in use on the solenoid). I did experiment with one IR laser diode rated with a lasing threshold of 1.4 A. However, the diode was faulty and would not lase for reasonably supplied amperages (up to 4 A).

CIRCUIT

The circuit below was designed using a 555 chip to pulse three 840 nm IRLEDs at 25 kHz. The output is picked up by a photodiode and amplified then fed into a computer for processing.

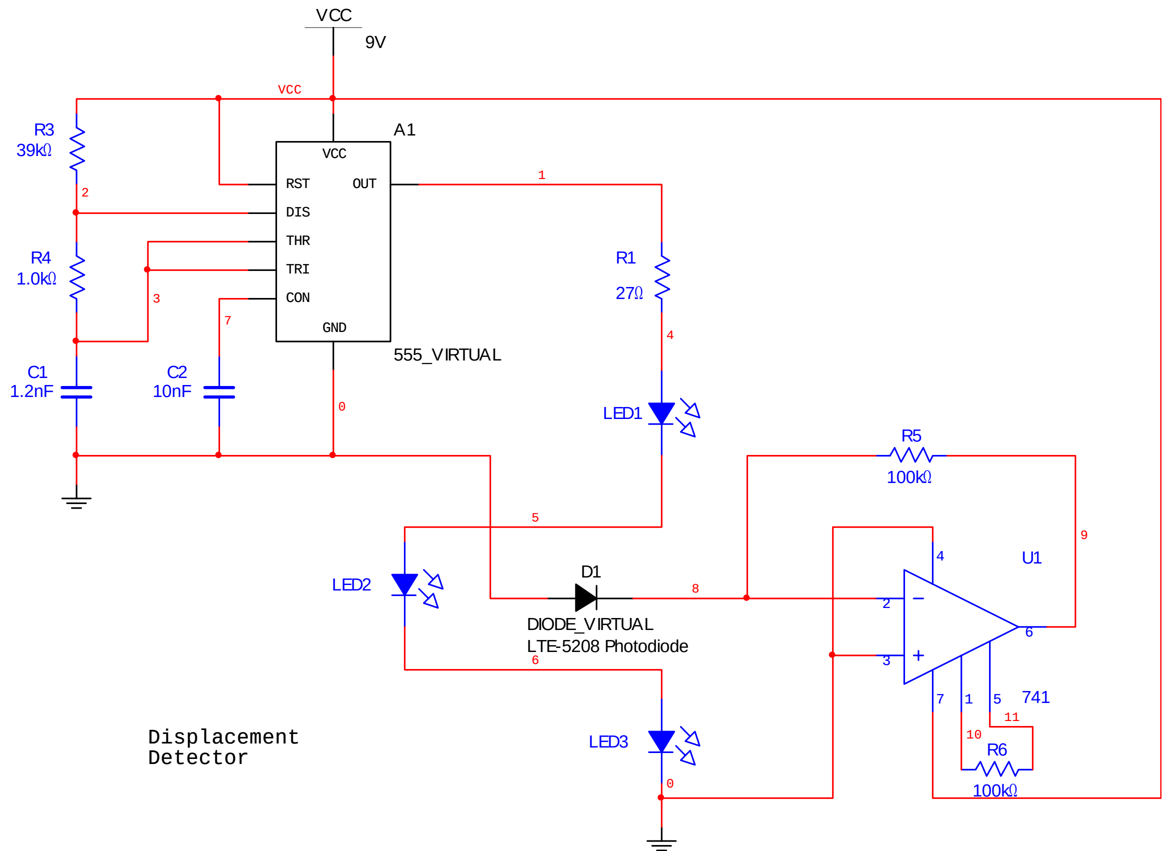

Figure 17: Position Sensor Circuit

The actual board was modified later on to a 20 kHz, approximate 50% duty cycle pulse train which allowed better response from the photodiode detector.

CONTROL

I. System Characterization:

To pick the optimal magnet for levitation one must consider its geometry. Consider a cylindrical magnet cut into thin lateral slices. Each slice contributes to the net flux of the entire system, but because the falloff of the magnetic field with respect to distance is faster then linear, each slice contributes less and less force between it and the permanent magnet in as it grows in distance from the core.

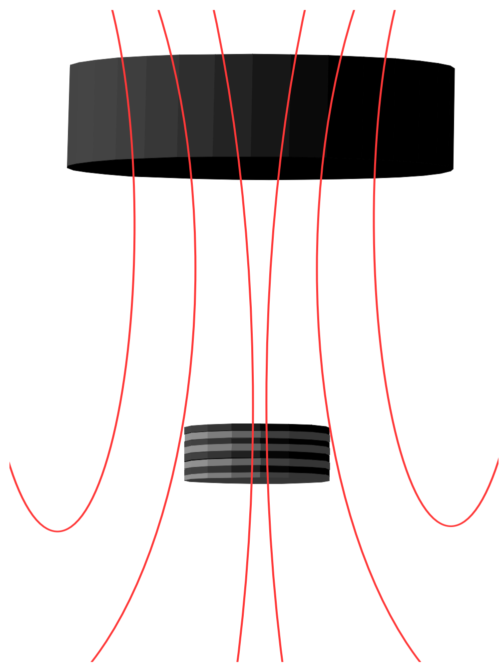

Figure 158: The Flux of two Permanent Magnets

Thus the added weight of each subsequent slice will grow faster than the total force.

Also notice that as the diameter of a slice levitating cylinder increases, it encompasses more field lines. Thus the force scales at approximately the same rate as the increase in weight for a magnet of larger surface area. Optimally, the best levitation magnet is as thin as possible with the same diameter (3”) as the core magnet.

Out of several different magnets, a 1.5” diameter by 1/8” thickness ND48 magnet was chosen as the levitator. A 3x1” N48 magnet similar to that in the core provided 50 times more force (at 72 times the mass). Although this magnet’s equilibrium floating position was about ½” less than that of the thinner magnet, its strength would allow for a larger, heavier induction coil and a greater payload. Another 1x1 N50 displayed a significant increase in strength per mass. It could float 10” at 0 amps and carry ample load. However, the latter two magnets both would require high current to achieve stability in regions above the equilibrium position nearer to the solenoid.

To measure the force between the magnets, fishing line was connected between a 239.8g wooden block and a 4.0g polystyrene block. The wooden block was placed on a scale and the levitation magnet floated beneath the polystyrene block. By reading the change in scale reading from the total component weights, the force between the magnets could be determined.

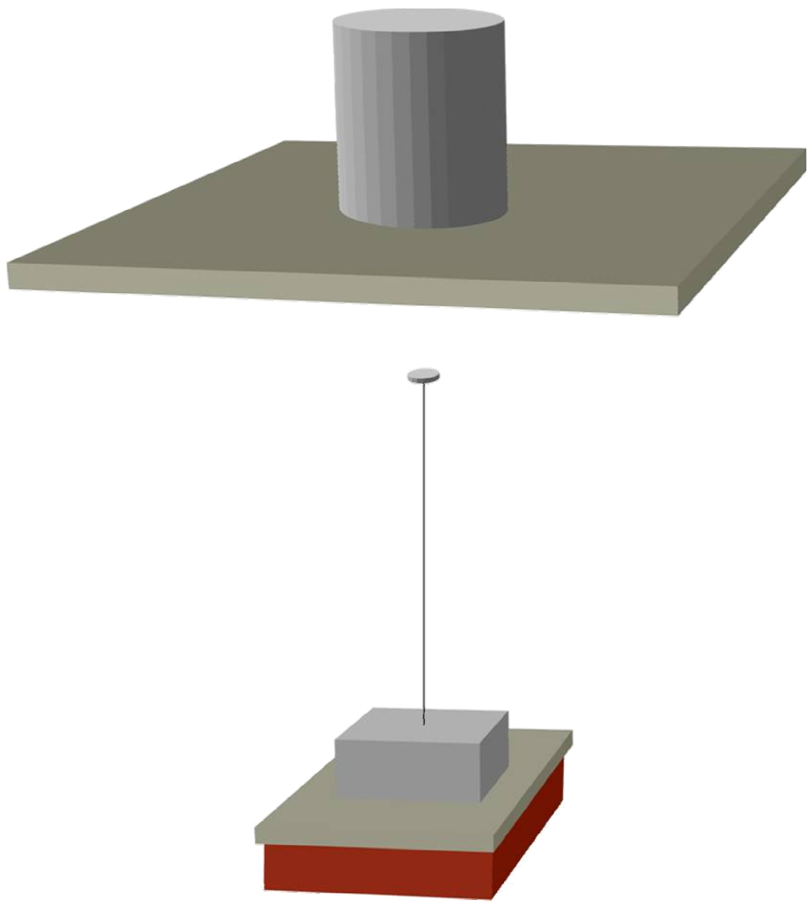

Figure 169: Force Measurement of System

By varying the current from -5 to 5V DC at set string lengths, the force contour vs. current and drop height could be determined.

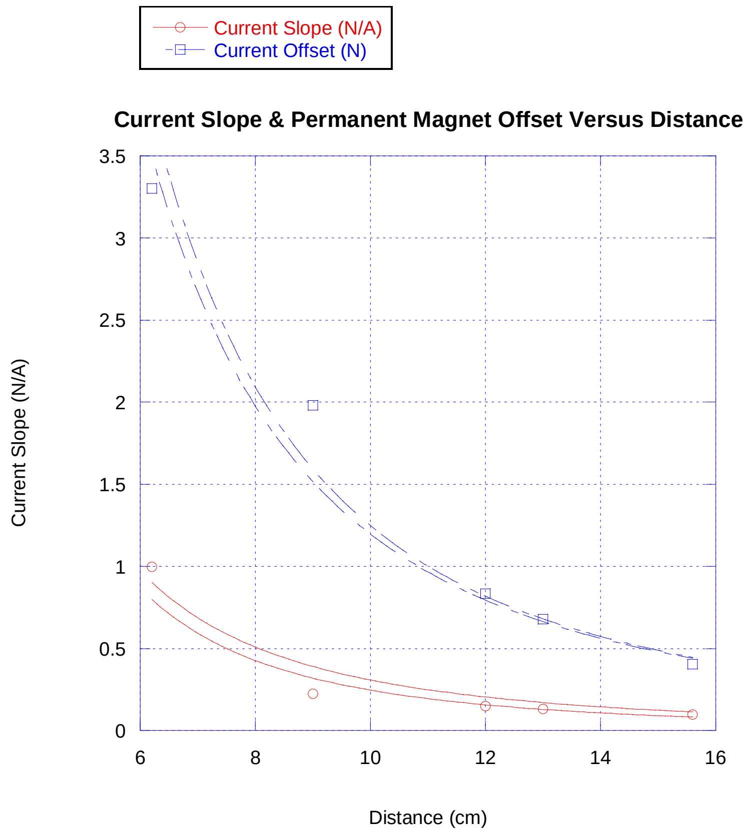

Figure 20: Falloff of the force due to the permanent magnet force and the slope of the force due to the solenoid.

Above are data points taken at 0 A (blue) and at a constant amperage (2.5 A, red) corresponding to the interaction with the permanent magnet in the core and the behavior of the solenoid separately. The lower fit fits all constant parameters in the function from Equation (). The upper fit forces the decay rate to $(z\text{-}m_{3,4})^{-9/4}$ as derived. I assume the second fit is more reliable as the second data point is obviously inaccurate and pulls each curve from its mark to the lower fit.

The magnetic force was found to be

$$F(z,i) = \frac{327i}{\left(z+1.44\right)^{9/4}} + \frac{18.5}{\left(z-2.53\right)^{9/4}} \tag{17}$$

considering all data. The functional force contour looks as such:

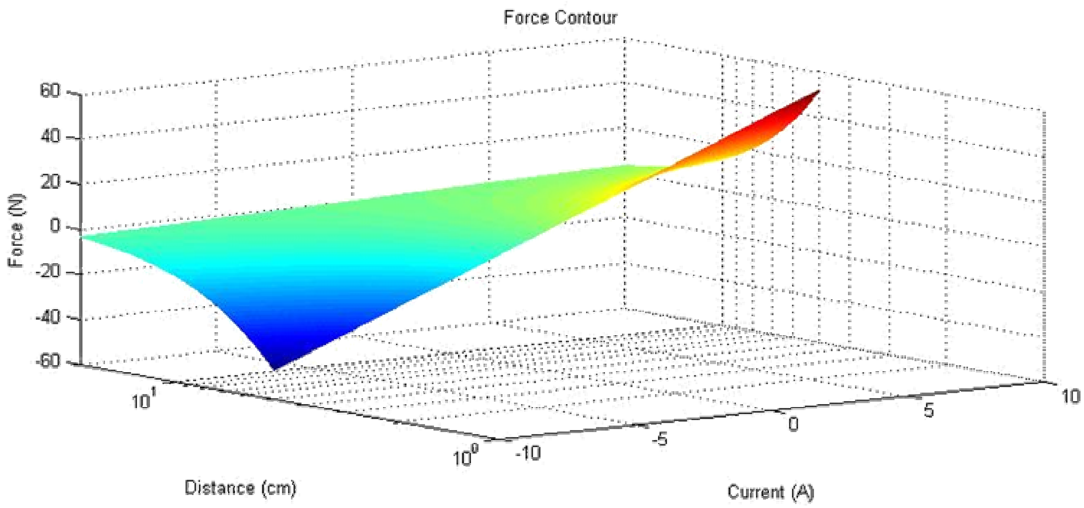

Figure 21: Force Contour of Levitation System

Empirically, we had found

$$f(i,z) = \frac{ai}{\left(z - z_1\right)^{9/4}} + \frac{b}{\left(z - z_0\right)^{9/4}} \tag{18}$$

Also,

$$f'(i,z) = -\frac{9b}{4\left(z - z_0\right)^{13/4}} - \frac{9ai}{4\left(z - z_1\right)^{13/4}} \tag{19}$$

where *z_1* is the distance from the electromagnet's effective center and *z_0* is the distance from the permanent magnet's center.

Expanding in a Taylor series we find the linearized expression about a position *p*:

$$\begin{aligned} f(z,i) &\approx f(p,0) + \frac{df}{dz}\Big|_{z=p,b=0}\left(z-p\right) + \frac{df}{di}\Big|_{z=p,b=0}\left(i-p\right) \\ &= \mathrm{b}\left(\mathrm{p}\text{-}\mathrm{z}_0\right)^{-9/4} + \frac{-9}{4} b\left(\mathrm{p}\text{-}\mathrm{z}_0\right)^{-13/4}\left(z-p\right) + a\left(\mathrm{p}\text{-}\mathrm{z}_1\right)^{-9/4} i \end{aligned} \tag{20}$$

Therefore,

$$f \approx A - B\left(z-p\right) + Ji$$

where

$$A = b\left(p - z0\right)^{-9/4}$$
$$B = \frac{9}{4} b\left(p - z0\right)^{-13/4}$$
$$J = a\left(p - z1\right)^{-9/4}$$

II. Equations of Motion near Position "*p*":

The equation of motion is

$$mg - F = m\ddot{z} - D\dot{z} \tag{21}$$

where z is the distance from the solenoid base and D is a damping term due to air resistance. This becomes

$$\ddot{z} + D\dot{z} - Bz = g - A - Bp - Ji \tag{22}$$

We'll substitute in the state variable $x = z + \frac{g - A}{B} - p$ to get rid of the offset on the input side of the equation.

Applying the Laplace Transform, the transfer function is

$$G_l(s) = -\frac{J}{s^2 + Ds - B} \tag{23}$$

II. COMPENSATOR DESIGN:

The system as a whole can be broken down as such:

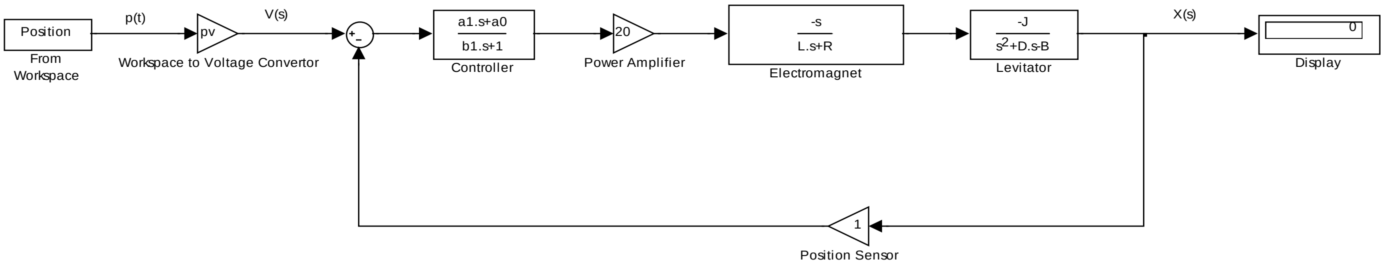

Figure 22: Control System Diagram

An input from the MatLab Workspace is converted into a voltage to be output to the system. The gain of the operational amplifier is set at about 20. The signal is sent to the electromagnet, the levitator responds, and the position from the detector is fed back into the controller to compensate the system.

The transfer function of the electromagnet's current in response to the applied voltage from the controller can be treated as an RLC circuit in series operation. We may also easily adjust the total capacitance by adding an external capacitor in series with the electromagnet to adjust for stability requirements. In this case, we will choose the total capacitance such that its contribution is negligible in order to reduce the order of the model. Assuming we connect the coil to the power supply in reverse sense (to get rid of unwanted negatives in the system transfer function), the electromagnet transfer function becomes

$$G_m(s) = -\frac{s}{Ls+R} \tag{24}$$

We will also set the gain of the power amplifier 20 and employ a phase-lead controller to improve stability. The open loop transfer function is then

$$G(s) = \frac{20J\left(a_1 s + a_0\right)}{L\left(b_1 s + 1\right)\left(Ls+R\right)\left(s^2 + D*s - B\right)} \tag{25}$$

and the characteristic equation of the open loop transfer function is

$$\begin{aligned} C(s) = b_1 L s^4 + \left(b_1 R + b_1 DL + L\right)s^3 + \left(b_1 DR + R + DL - Bb_1 L + 20a_1 J\right)s^2 \\ \left(DR \text{ - } Bb_1 R \text{ - } BL + 20a_o J\right)s - BR \end{aligned} \tag{26}$$

To satisfy the Routh-Hurwitz stability criterion we can quickly see that b_1 must be negative in order for all coefficients of the characteristic equation to match. At 10 cm, with a solenoid inductance of .962 H and resistance of 14 Ohms, the root locus of the uncompensated open loop transfer function looks as such:

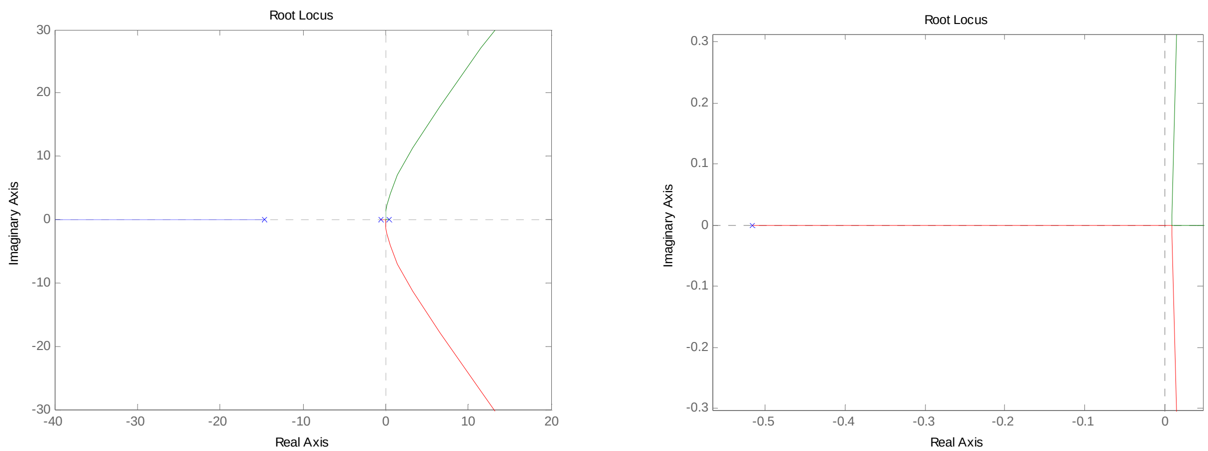

Figure 23: Root Locus of Uncompensated System

We have also approximated the damping coefficient D is negligible for ease of calculation.

The controller is decided to be phase-lead (as shown in the overall system above) to account for the poles in the right half plane of the complex plot. We will pick our new pole at -0.4 ± 0.0j based on the blowup above to stabilize the system. Because we are not so concerned with the speed of the system, we will choose controller values fairly arbitrarily to lead to simplistic calculation. Thus, we will also choose a_0 = 1. For any point about which the system transfer function is linearized, controller values a_1 and b_1 are calculated according to

$$a_1 = \frac{\sin(-0.4+0.4j) + \left|G_p(-0.4+0.4j)\right| \sin\left(angle\left(-0.4+0.4j\right) - angle\left(\left|G_p(-0.4+0.4j)\right|\right)\right)}{\left|-0.4+0.4j\right| \left|G_p(-0.4)\right| \sin\left(angle\left(\left|G_p(-0.4+0.4j)\right|\right)\right)}$$

$$b_1 = \frac{\sin\left(angle\left(-0.4+0.4j\right) + angle\left(\left|G_p(-0.4+0.4j)\right|\right)\right) + \left|G_p(-0.4+0.4j)\right| \sin\left(-0.4+0.4j\right)}{-\left|-0.4+0.4j\right| \sin\left(angle\left(\left|G_p(-0.4+0.4j)\right|\right)\right)}$$

(1)

For this particular example we can see that the step response is very slow and the steady state error is almost 5 cm, although simulation shows stability.

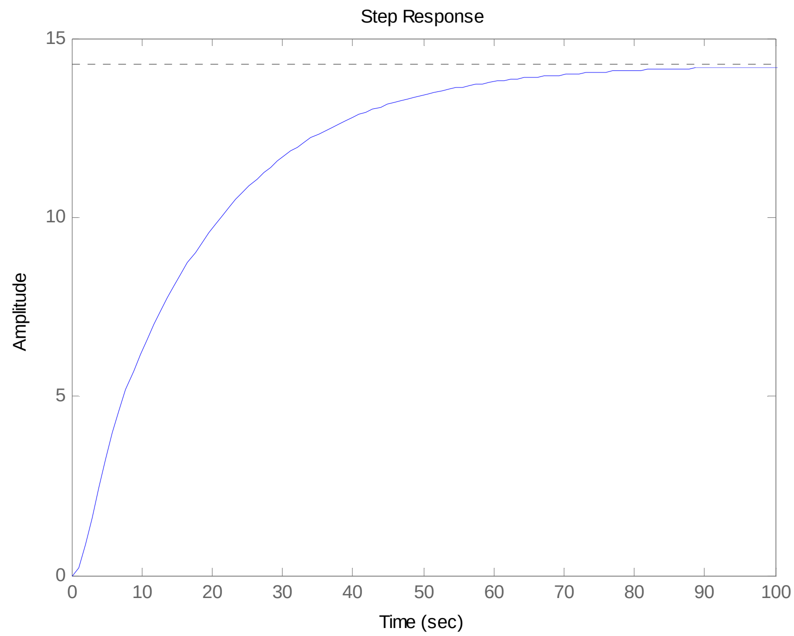

Figure 24: Simulated Step Response of Compensated System

In implementation this configuration is not permanently sable and the levitation magnet will eventually fall to the ground. In attempts to speed up the system by choosing different poles, the general result is the opposite, and the levitator flies to the solenoid. This is most likely due to the extreme nonlinearity of the system away from the linearized position.

III. IMPLEMENTATION:

An input from the PCI 1200 Data Acquisition System is fed into a Simulink Real Time Workshop control system. The linearized position's corresponding variables are calculated and proper controller configuration implemented on the fly.

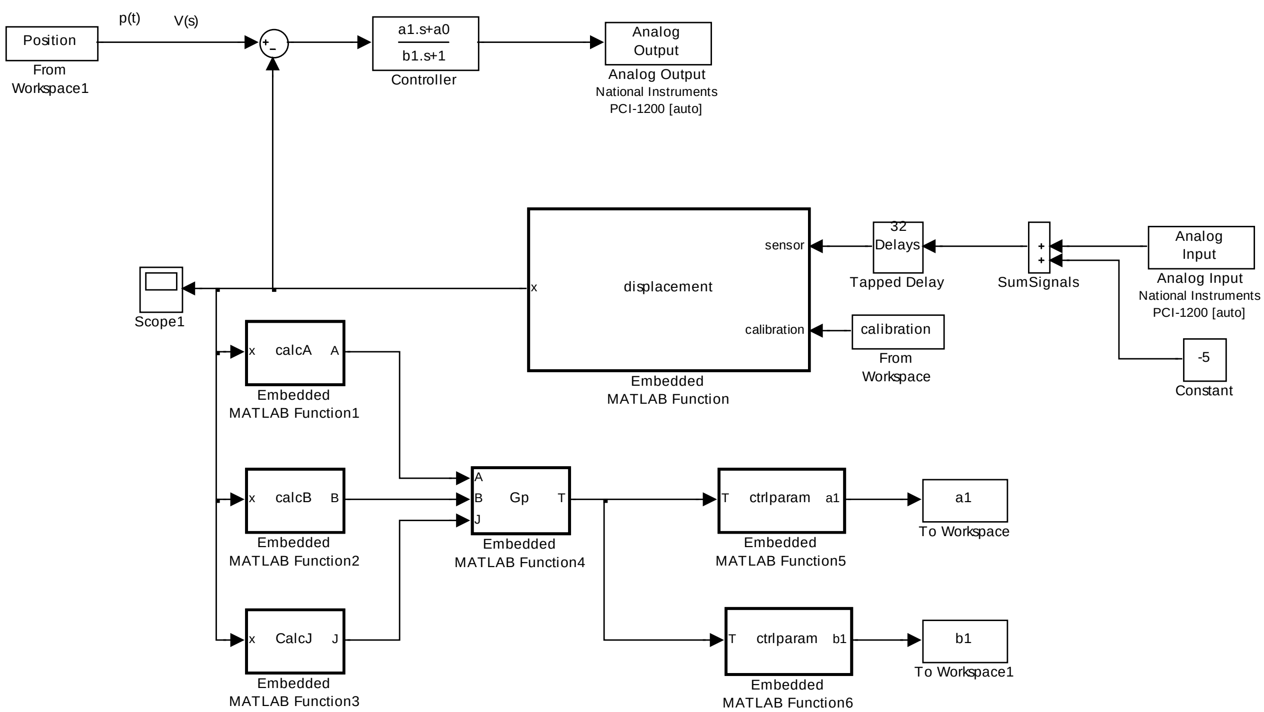

Figure 25: Simulink Workspace Layout of Control System

The controller output (-5 to 5V analog) is sent to the push-pull amplifier that drives the system and attempts to hold the system in the desired equilibrium position. The settling time is ignored in calculation as we do not require high speed – only high accuracy – to prevent disturbances into nonlinear regions.

Unfortunately, disturbances driving the levitation magnet closer to the permanent magnet in the solenoid increase the necessary power from the amplifier beyond its limit to drive the levitator back down to equilibrium. The problem could also rest within the control system as I have not had the time within the duration of this project to optimize it.

Because of the limiting driving frequency of the Kepco bipolar op-amps I was originally using, I was only able to obtain 1/200 of the supply voltage in a light, 4" diameter coil of 100 windings one foot in distance from the solenoid. It would be interesting to see if reasonable voltage could be obtained from a faster power supply considering the fact that induction is directly proportional to driving frequency. Of course, driving the solenoid at a high frequency would also have the negative effect of increased impedance within the winding, requiring a more powerful power supply. As it is now, a battery mounted on the floatation device could easily be recharged in close proximity to the solenoid before traveling to its desired position.

DISCUSSION & CONCLUDING REMARKS

In simulation, a phase-lead controller was able to stabilize and control the magnetic levitation system assuming ideal position and derivative feedback with an ideal power supply. In practice, stability was not so easy to obtain. Because of the strong position dependence of the magnetic field, a power supply must be able to respond with ample current within the time constant of the system. The two Kepco bipolar operational amplifiers I was originally using could only supply 5.6A when 10A would have been the tolerable minimal. These op-amps were also poor at driving the large inductive load required to levitate the object. Switching times only approached the 20 kHz region while the solenoid was designed and built to resonate around 10 MHz.

At 20 kHz, the system can only induce 1/200 of the supply voltage into a small 4" coil of 100 turns. To curb the power supply issue I have built my own push-pull amplifier. I am now able to drive the solenoid up to 1 MHz with reasonable current, although time has not permitted me to test power by induction at this frequency.

Modification to the solenoid design could also significantly loosen the requirements on the power supply. The field strength of the solenoid at a given current can be improved by increasing winding density. Thus, constructing an 8" outer diameter spool with a one to two inch inner diameter could greatly boost performance. In order to maintain the same DC resistance of a solenoid with higher winding density, the spool length would have to be shortened from 7" to two or three inches as well.

The smaller size of the spool's inner diameter would also allow other benefits. Because of the decrease in inner diameter and length, a solid piece of Hyperco Alloy 50 could be used as the core for an affordable price. Also, the decreased length would allow one to put the permanent magnet on the backside of the spool. With the permanent magnet at the front (nearest to the levitating magnet) the performance of the core was greatly reduced because its effective center was moved farther away from the levitating magnet. However, the permanent magnet could not be moved to the back of the spool because the falloff of its field through the insubstantial core is too great and the field would be significantly diminished at the front of the electromagnet. On the back of a shorter solenoid with a solid core, the decay of the DC field would be minimal while the electromagnet's performance would be significantly increased by the nearness of the core.

Unfortunately, decreasing the length of the solenoid also increases its inductance. Based on the recommended geometry for a new solenoid described above, this inductance would increase threefold upon shortening of the solenoid. However, this could be curbed by a factor of eleven simply by wiring layers of winding in parallel. A 5V, 10A power supply would be more than sufficient for the task of driving this solenoid.

It may seem like levitation and power by induction costs a great deal of power, but it must be realized that near the median operating distance as dictated by the DC field of the permanent magnets, minimal power is supplied. General power is spent driving small perturbations back to equilibrium only. The high wattage is necessitated by the initial dropping the permanent magnet to its resting position. In a worst case scenario, it might take 1000W to drop a 1x1" neodymium magnet 10cm. However, as soon as the field is cancelled the magnet will begin to fall at 9.8m/s. Thus it will only take one hundredth of a second to fall the 10cm. This is a total energy consumption of only 10J (1000W*1/100s)! After this, the required power should be far less. Of course, high power is still needed for floating an object especially near or far away from the solenoid.

This project has showed that simultaneous levitation and power by induction is a feasible method for controlling a wireless device through space. Although neither controlled levitation nor efficient power by induction was successfully implemented, rules for constructing a better system were made clear. Hopefully, this project will be able to be extended upon in the years to come.

ACKNOWLEDGEMENTS

I would like to give special thanks to my advisor Erik Cheever, Carl Grossman, Grant Smith, and Ed Jaoudi for their support and feedback. I would also like to hank Jim Holdeman and Steve Palmer whose work was indispensable in constructing the electromagnet.

REFERENCES

1. Callister, William D. Jr. *Materials Science and Engineering*. Hoboken, NJ: John Wiley & Sons, 2003.

2. Griffiths, David J. *Introduction to Electrodynamics*. Upper Saddle River, NJ: Prentice-Hall Inc., 1999.

3. Ogata, Katsuhiko. *System Dynamics*. Upper Saddle River, NJ: Prentice-Hall Inc., 1998.

4. Phillips, Charles L. & Royce, D. Harbor. *Feedback Control Systems*. Upper Saddle River, NJ: Prentice-Hall Inc., 2000.

5. Purcell, Edward M. *Electricity and Magnetism*. New York, NY: McGraw-Hill Science, 1984.

APPENDIX

CONTENTS

A. Sample Code

B. Force Data

C. Neodymium Magnet Properties

D. Solenoid Properties at 4.5A

E. Data Sheets

SAMPLE CODE

Wire Gauge Scrip:

Java Script:

```
public class maxVoltage {
    public static void main(String[] args) {

        double N=2500.0;
        double[] R={0.9989, 1.26, 1.588, 2.003, 2.525, 3.184, 4.016, 5.064, 6.385, 8.051, 10.15,
12.8, 16.14};
        double[] d={2.58826, 2.30378, 2.05232, 1.8288, 1.62814, 1.45034, 1.29032, 1.15062,
1.02362, 0.91186, 0.8128, 0.7238, 0.64516};
        double[] Vmax=new double[R.length];
        double[] L=new double[R.length];
        double[] Rtotal=new double[R.length];
        double[] width = new double[R.length];
        double Ampl=4.0;

        for(int i = 0; i< R.length; i++) {
            Rtotal[i]=(14.5*N*R[i])/12000;
        }

        double pi=Math.PI;
        double omega=2*pi*1000.0;
        //System.out.println(pi);
        double u=4*pi*1E-7;
        //System.out.println(u);
```

```
for (int i = 0; i < R.length; i++) {
    L[i]=u*N/4*pi*Math.pow((8.0*0.0254),2);
    width[i]=N*Math.pow((d[i]*0.0393700787),2)/6.25;
}
for (int i = 0; i < R.length; i++) {
    double arctanterm=Math.atan(-L[i]*omega/Rtotal[i]);
    double costerm=Math.cos(arctanterm);
    double sinterm=Math.sin(arctanterm);
    Vmax[i]=Ampl*(Rtotal[i]*costerm-L[i]*omega*sinterm);
}
for (int i = 0; i < R.length; i++) {
    System.out.println(Vmax[i]);
}
System.out.println("min omega");
for (int i = 0; i < R.length; i++) {
    System.out.println("  "+ (10*L[i]/Rtotal[i]));
}
System.out.println("resistance");
for (int i = 0; i < R.length; i++) {
    System.out.println("  "+ (Rtotal[i]));
}
System.out.println("width");
for (int i = 0; i < R.length; i++) {
    System.out.println("  "+ (width[i]));
}
```

```
    }
}
```

Position Sensing:

```
function h = displacement(sensor,calibration)
% Takes unfiltered signal from position sensor every 32 data points
(.64 ms).
% Determines position and converts to control voltage.

        Fs = 50000;                                                    %Sample
Frequency
        clk = 19980;                                                   %Expected
Signal Frequency = 19.98 kHz
        t = (0:length(sensor)-1)*(1/Fs);
%time step vector for 34 points
        tnew = 0:t(length(t)/2^13-1:t(length(t));
%time step vector with 2^13 points
        signal = interp1(t,sensor,tnew,'spline');
%interpolate data for better resolution
        signalfft = fft(signal);                                  %Fourier xform
with 2^13 data points
        newFs = 1/(t(length(t))/(2^13));
        normalfreq = linspace(0,0.5,2^13/2);
        f = normalfreq(2)*newFs;
%f is the data separation in Hz
        pwr = abs(signalfft(round((clk-
80)/f)):signalfft(round((clk+120)/f))).^2;  %Power spectrum of the
signal near 19.98 kHz
        h=calibration*max(pwr);                                        %Determines
max power and scales to 0-5V
end
```

FORCE DATA:

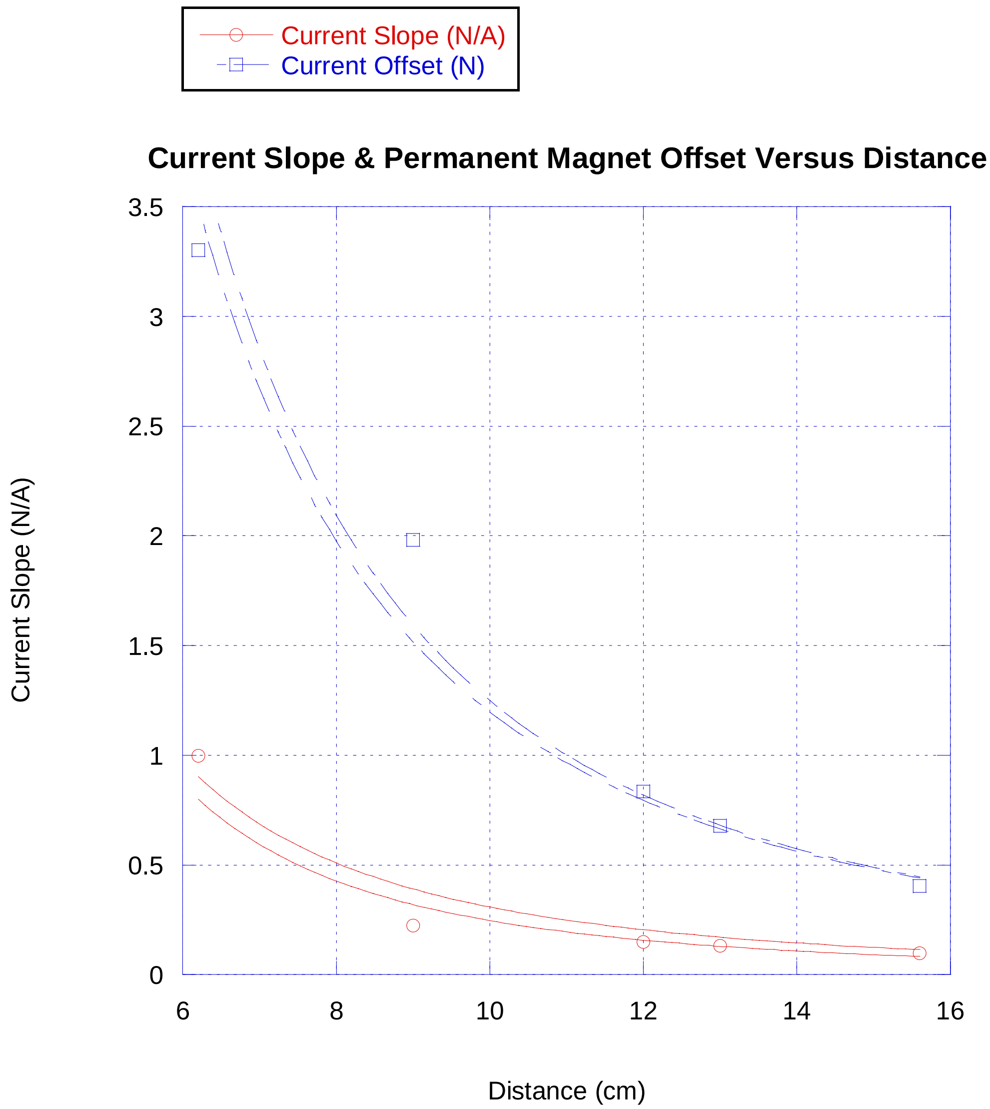

Current Slope (N/A)
Current Offset (N)
Current Slope & Permanent Magnet Offset Versus Distance
3.5
3
2.5
2
1.5
1
0.5
0
Current Slope (N/A)
6
8
10
12
14
16
Distance (cm)

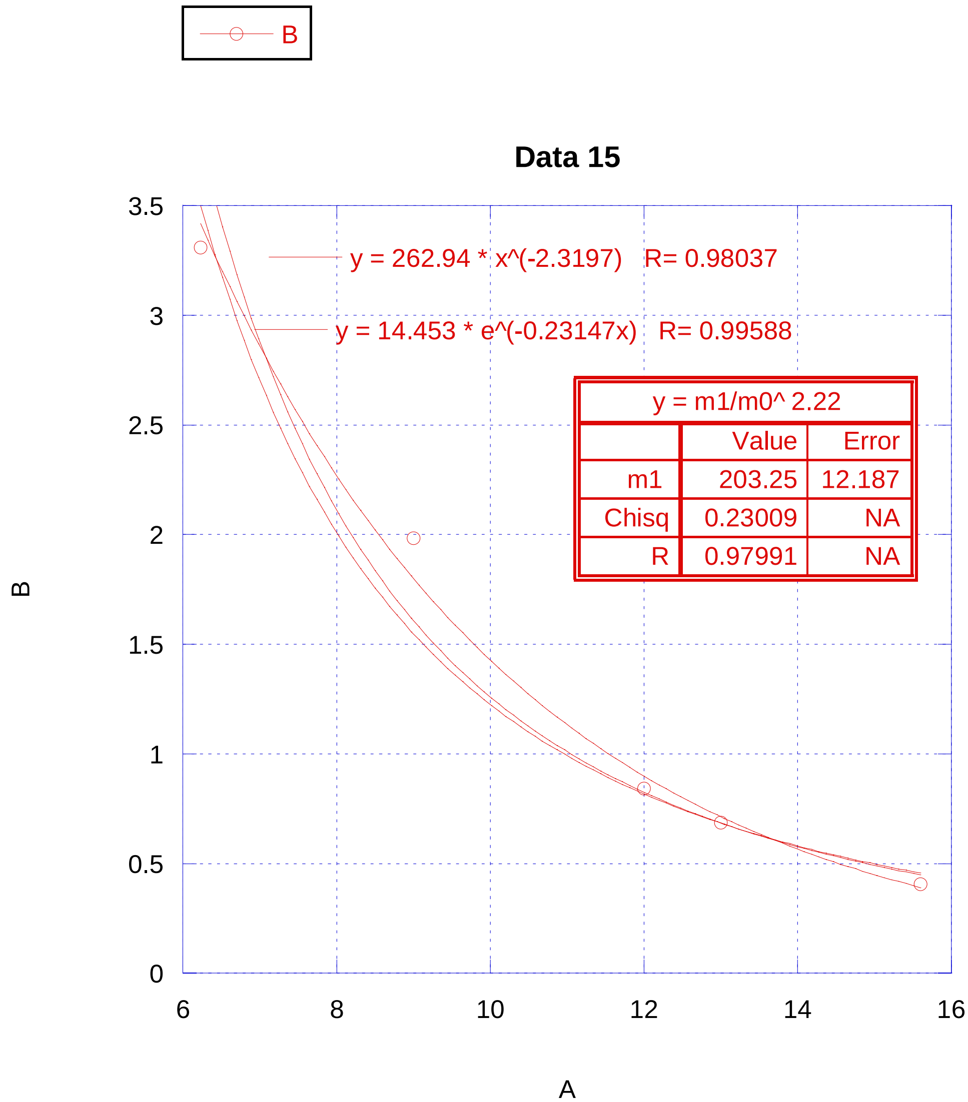
B
Data 15
y = 262.94 * x^(-2.3197) R= 0.98037
y = 14.453 * e^(-0.23147x) R= 0.99588
y = m1/m0^ 2.22
Value
Error
m1
203.25
12.187
Chisq
0.23009
NA
R
0.97991
NA
3.5
3
2.5
2
1.5
1
0.5
0
6
8
10
12
14
16
B
A

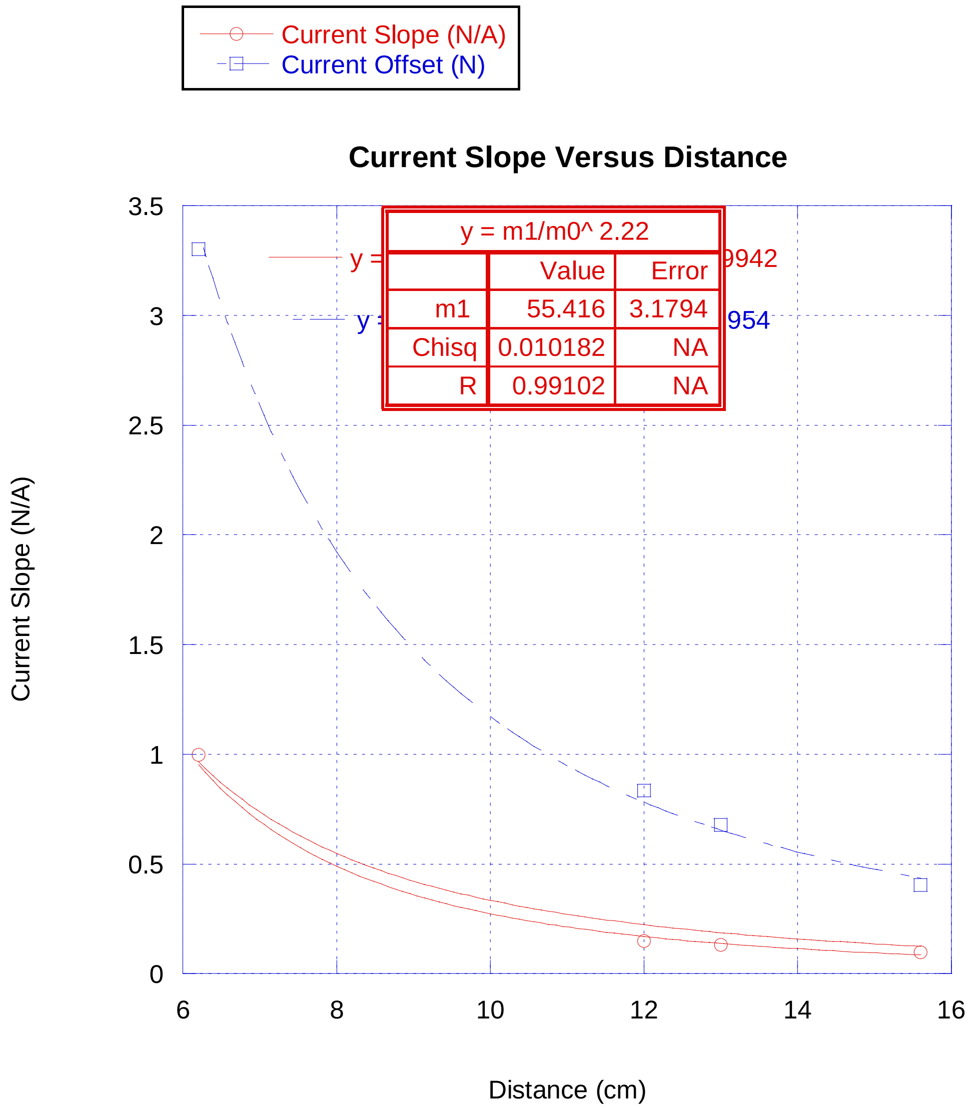
Current Slope (N/A)
Current Offset (N)
Current Slope Versus Distance
y = m1/m0^ 2.22
Value
Error
m1
55.416
3.1794
Chisq
0.010182
NA
R
0.99102
NA
9942
954
3.5
3
2.5
2
1.5
1
0.5
0
6
8
10
12
14
16
Current Slope (N/A)
Distance (cm)

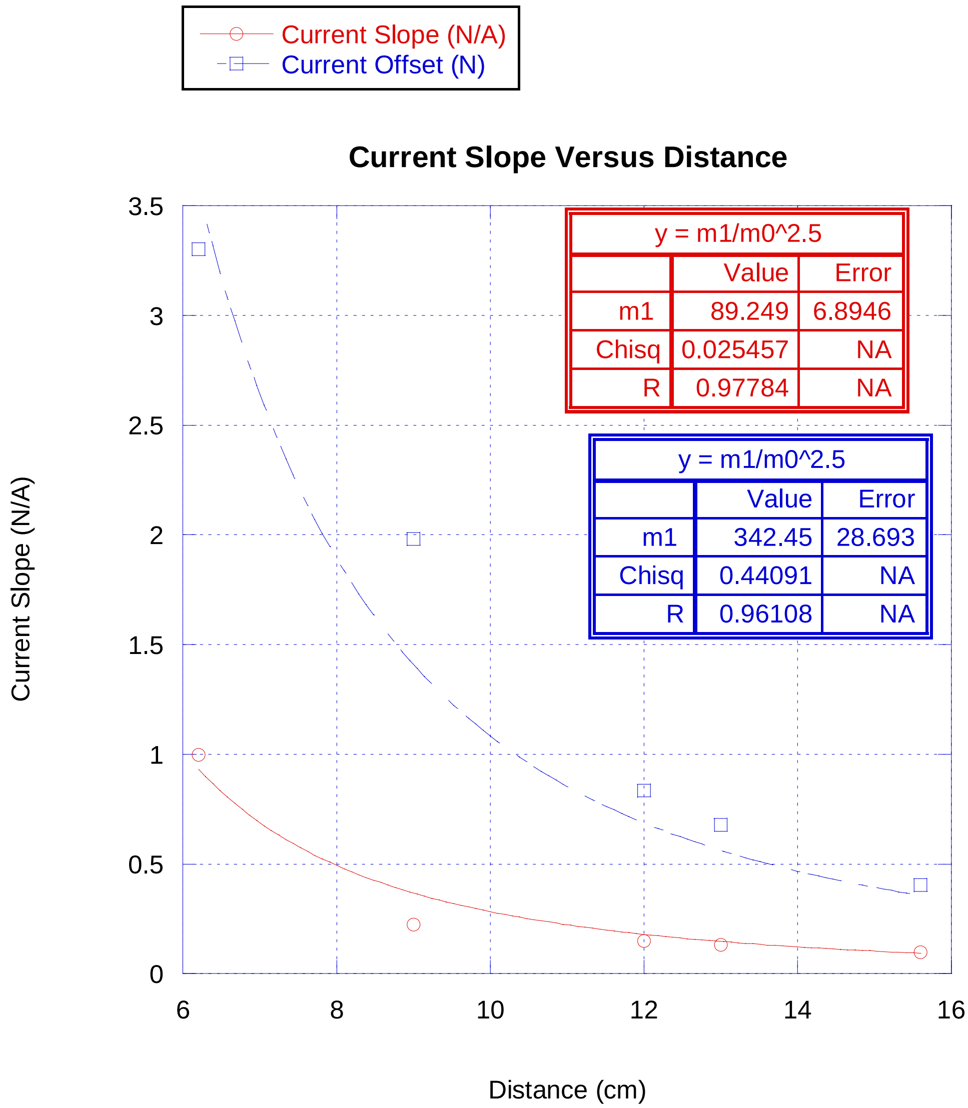

Current Slope (N/A)
Current Offset (N)
Current Slope Versus Distance
y = m1/m0^2.5
Value
Error
m1
89.249
6.8946
Chisq
0.025457
NA
R
0.97784
NA
y = m1/m0^2.5
Value
Error
m1
342.45
28.693
Chisq
0.44091
NA
R
0.96108
NA
Current Slope (N/A)
3.5
3
2.5
2
1.5
1
0.5
0
6
8
10
12
14
16
Distance (cm)

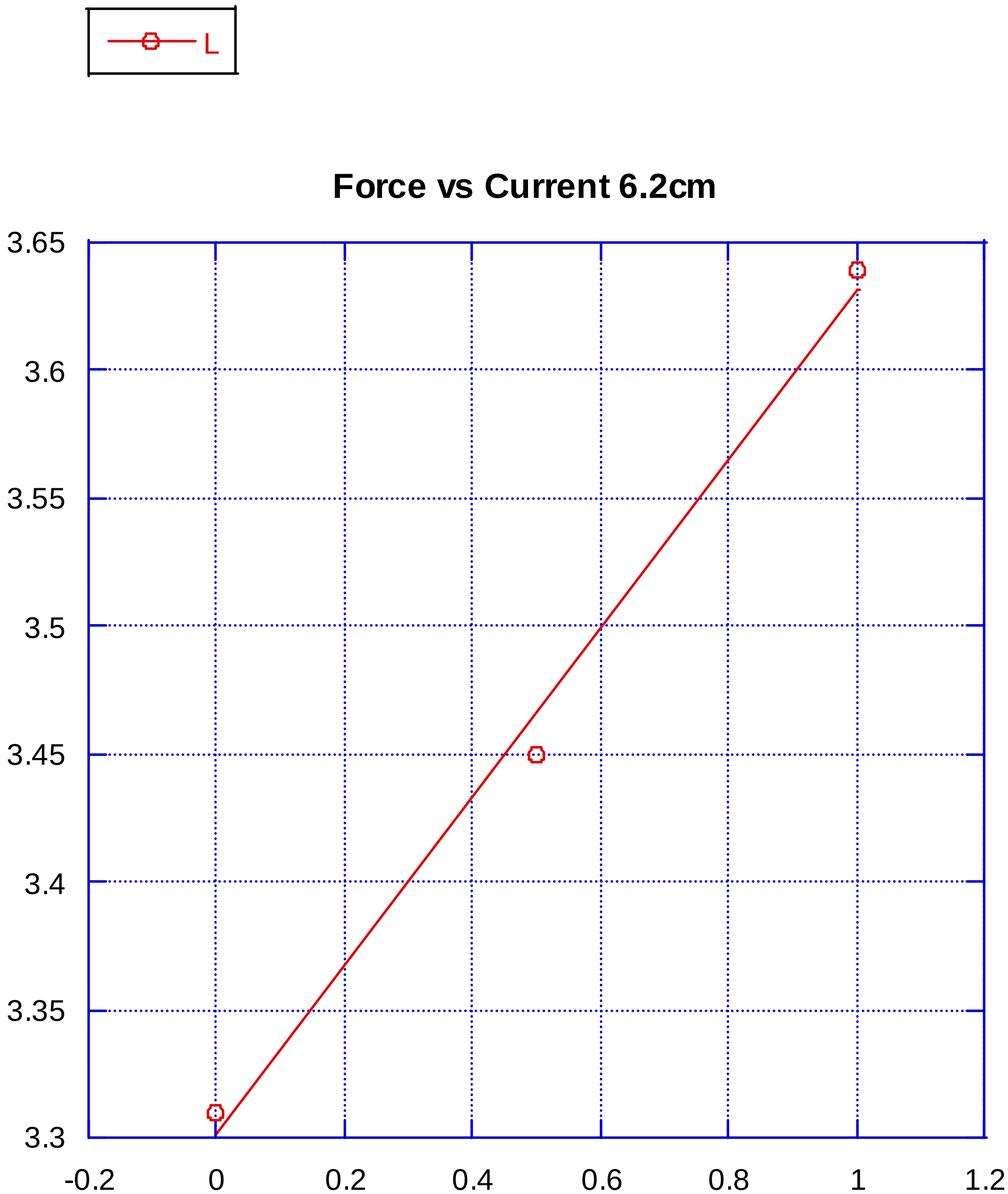
L
Force vs Current 6.2cm
3.65
3.6
3.55
3.5
3.45
3.4
3.35
3.3
-0.2
0
0.2
0.4
0.6
0.8
1
1.2

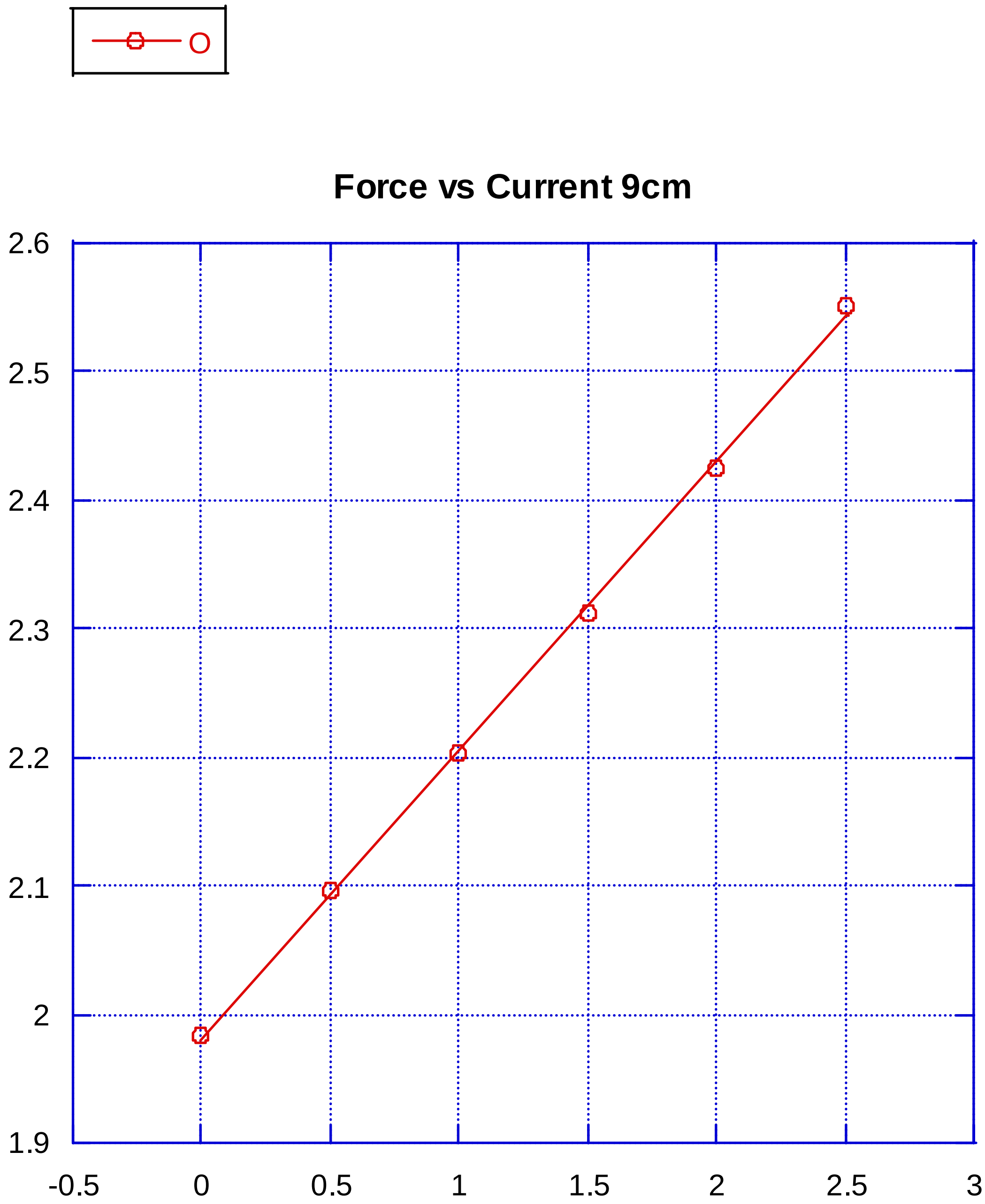
O
Force vs Current 9cm
2.6
2.5
2.4
2.3
2.2
2.1
2
1.9
-0.5
0
0.5
1
1.5
2
2.5
3

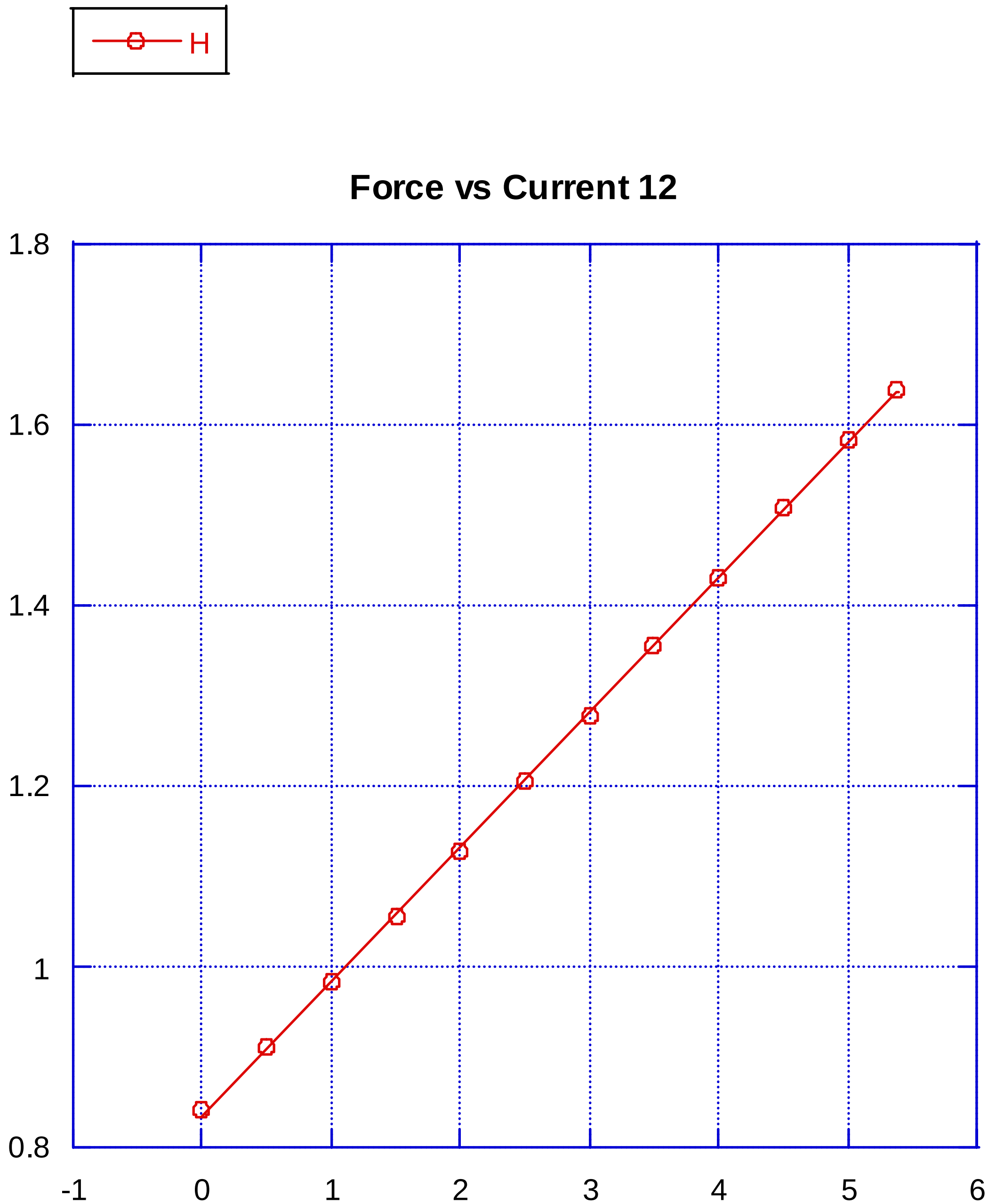
H
Force vs Current 12
1.8
1.6
1.4
1.2
1
0.8
-1
0
1
2
3
4
5
6

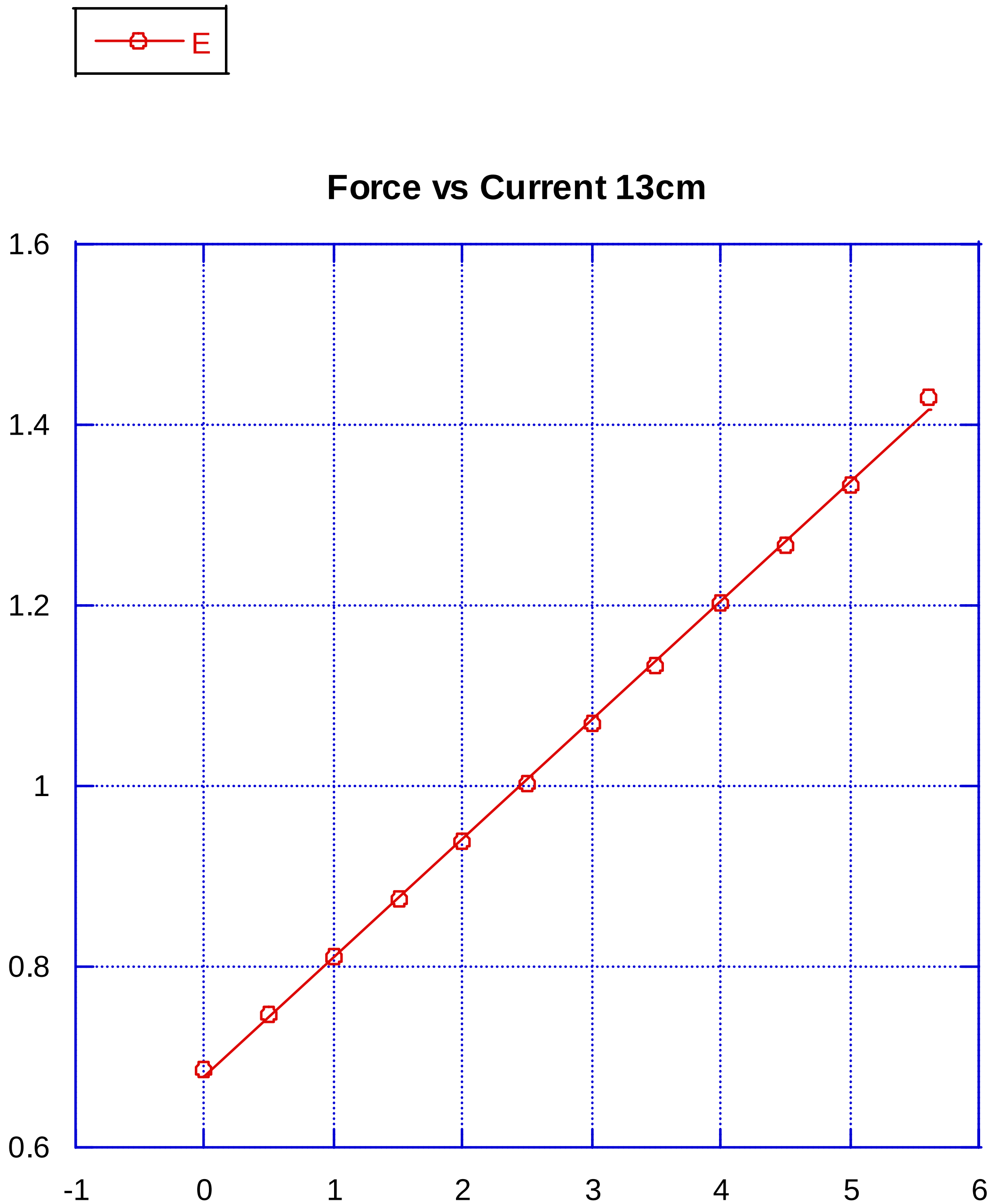
E
Force vs Current 13cm
1.6
1.4
1.2
1
0.8
0.6
-1
0
1
2
3
4
5
6

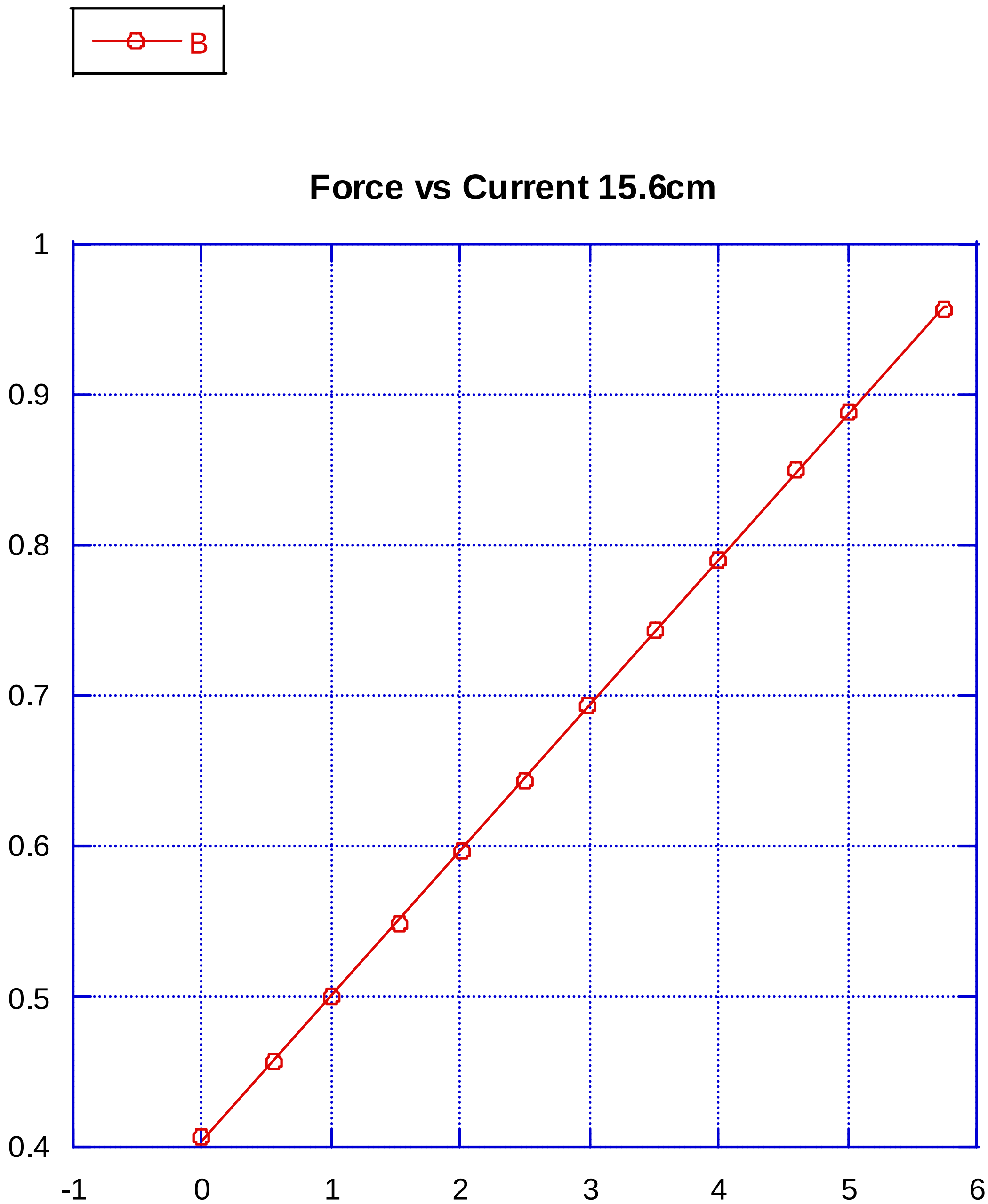
B
Force vs Current 15.6cm
1
0.9
0.8
0.7
0.6
0.5
0.4
-1
0
1
2
3
4
5
6

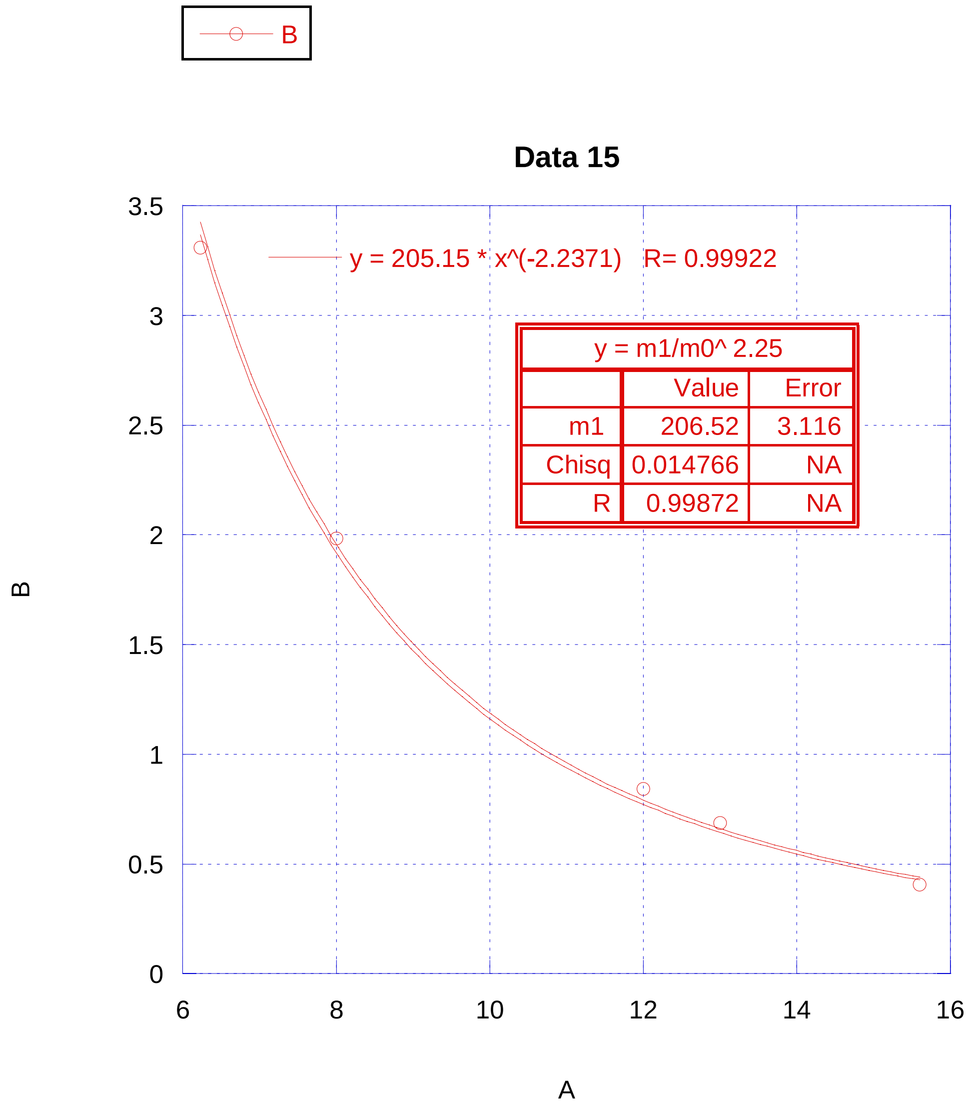
B
Data 15
y = 205.15 * x^(-2.2371) R= 0.99922
y = m1/m0^ 2.25
Value
Error
m1
206.52
3.116
Chisq
0.014766
NA
R
0.99872
NA
3.5
3
2.5
2
1.5
1
0.5
0
6
8
10
12
14
16
B
A

NEODYMIUM MAGNET PROPERTIES:

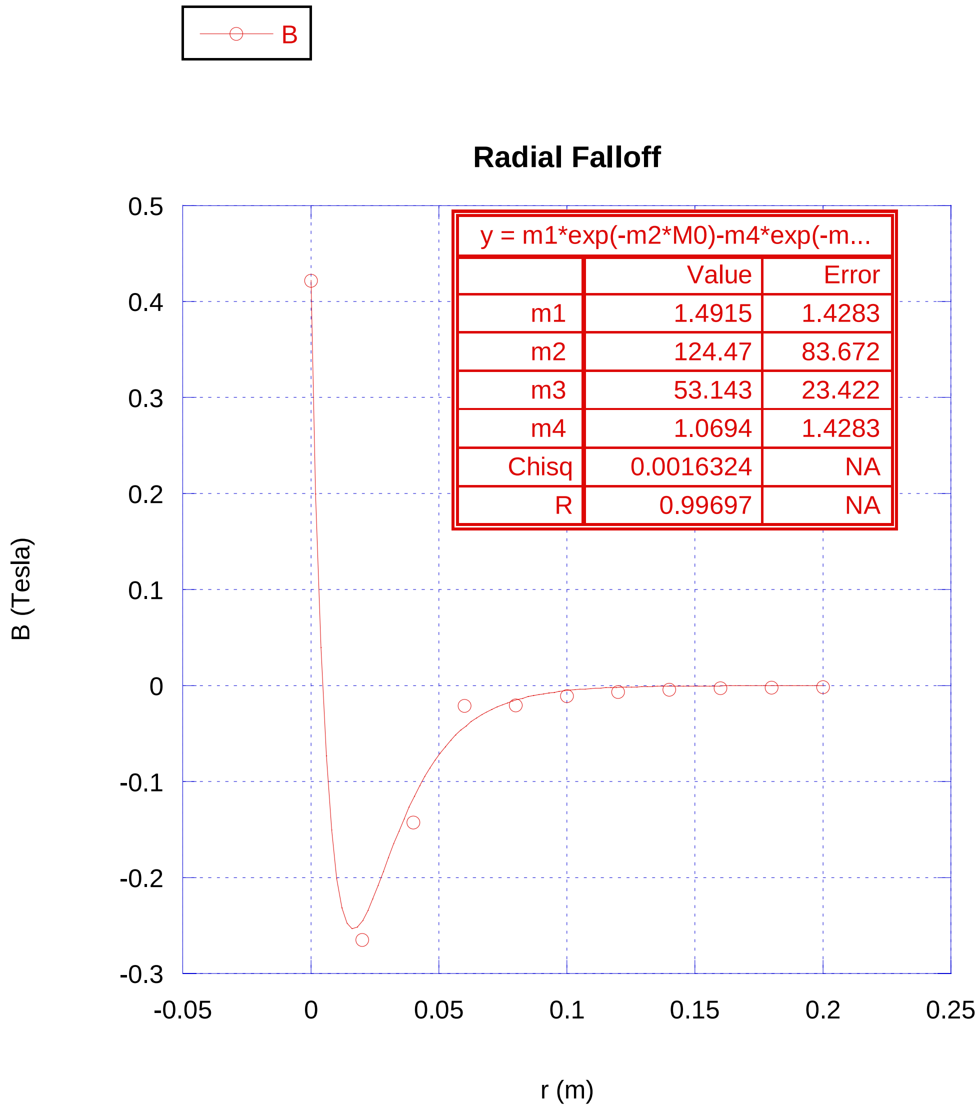

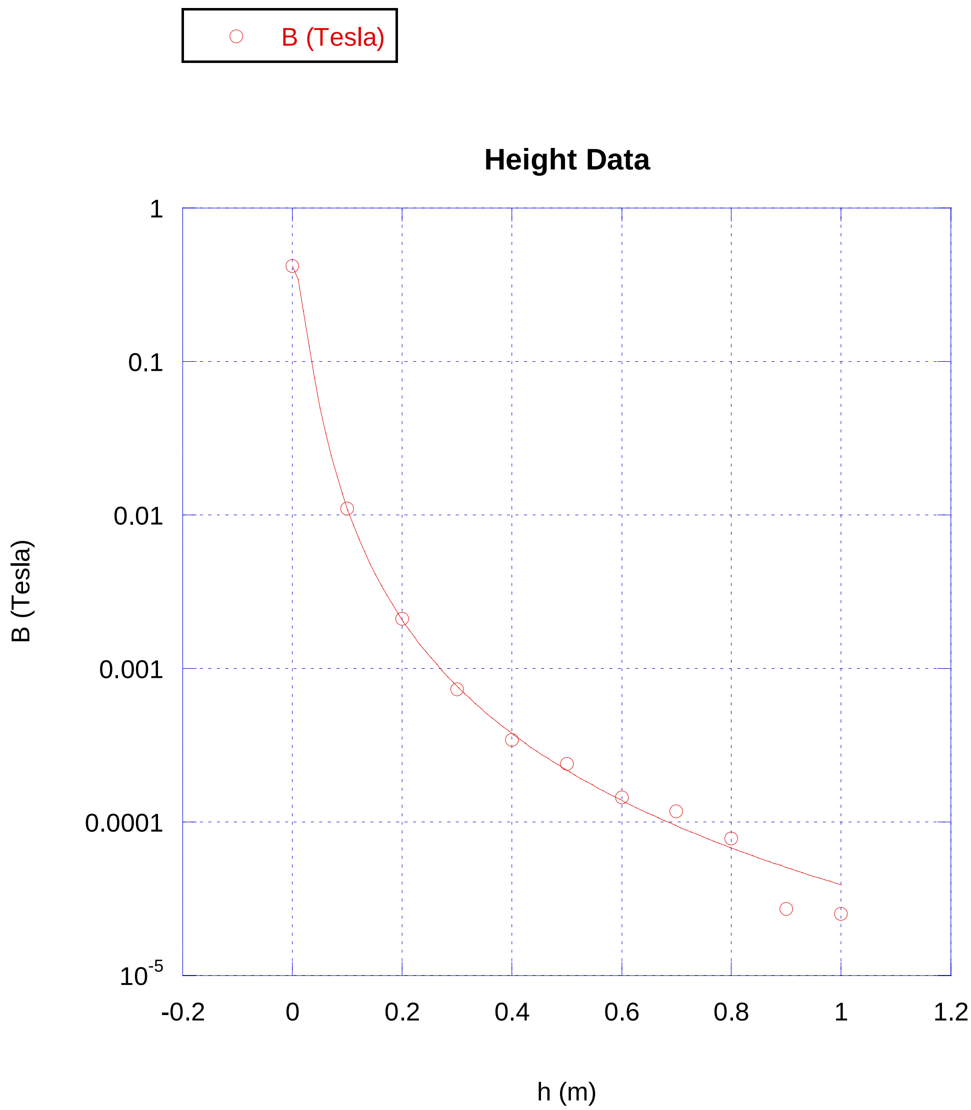
B (Tesla)
Height Data
1
0.1
0.01
0.001
0.0001
10-5
B (Tesla)
-0.2
0
0.2
0.4
0.6
0.8
1
1.2
h (m)

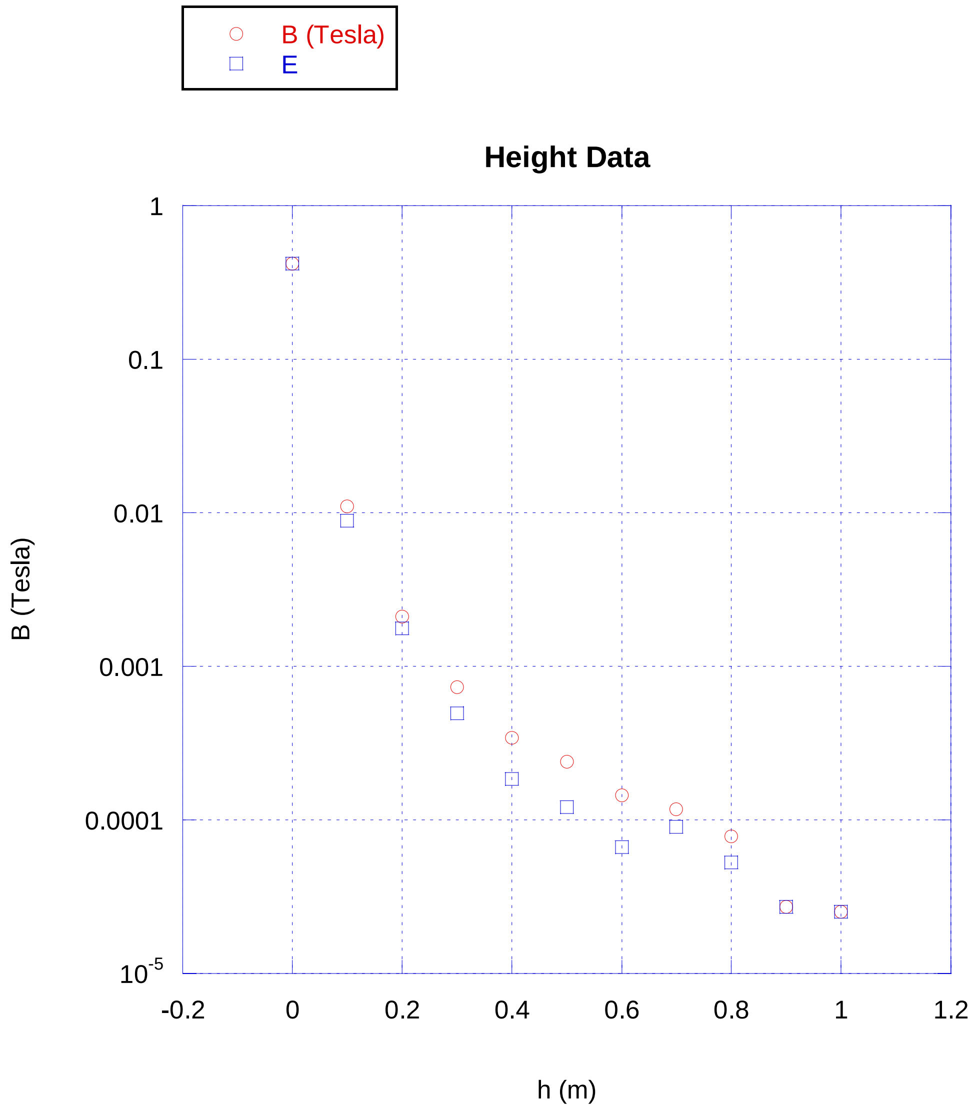

Figure 17

Neodymium Magnetic Field (h=0 at surface, N+) in Tesla:

$$B(r,h) = 12.83\times10^{-5}\,\frac{\left(e^{-124.5r} - .7170e^{-53.14r}\right)}{\left(5.589\times10^{-4} + h^{2}\right)^{-5/4}}$$

SOLENOID PROPERTIES AT 4.5A:

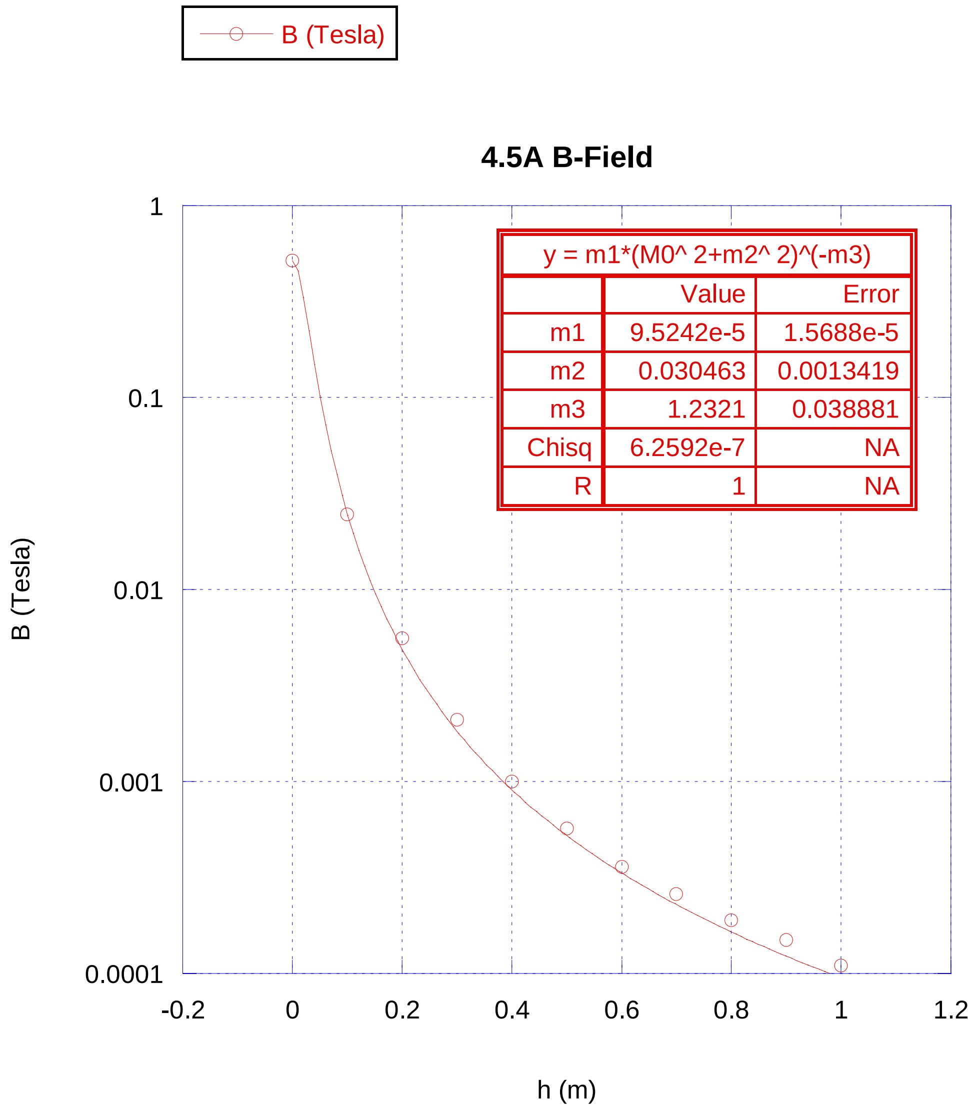

Falloff of solenoid at 4.5 A.

Vmax Min Nat Freq Width Guage Resistancs (Ohms)

12.339	0.00033763	4.1534	10.000	3.0175
15.439	0.00026766	3.2906	11.000	3.8063
19.358	0.00021238	2.6115	12.000	4.7971
24.338	0.00016838	2.0736	13.000	6.0507
30.618	0.00013357	1.6435	14.000	7.6276

38.558	0.00010592	1.3042	15.000	9.6183
48.594	8.3978e-05	1.0323	16.000	12.132
61.244	6.6599e-05	0.82084	17.000	15.297
77.195	5.2820e-05	0.64964	18.000	19.288
97.317	4.1890e-05	0.51552	19.000	24.321
122.67	3.3227e-05	0.40960	20.000	30.661
154.69	2.6348e-05	0.32481	21.000	38.667
195.04	2.0896e-05	0.25806	22.000	48.756

DATA SHEETS:

LED

Infrared LED
L2656 series

High power GaAlAs infrared LED

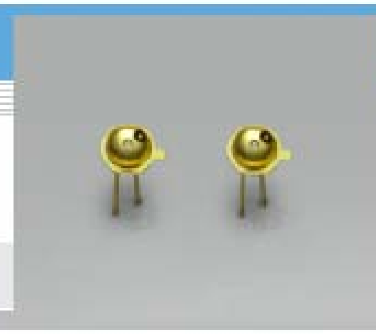

Features

- High radiant output power
- High reliability

Applications

- Optical switch
- Automatic control system

■ Absolute maximum ratings (Ta=25 °C)

Parameter	Symbol	Condition	Value	Unit
Forward current	I_F		80	mA
Reverse voltage	V_R		5	V
Pulse forward current	I_{FP}	Pulse width=10 µs Duty ratio=1 %	1.0	A
Operating temperature	Topr		-30 to +85	°C
Storage temperature	Tstg		-40 to +100 *	°C

* Guaranteed to resist temperature cycle test of up to 5 cycles.

■ Electrical and optical characteristics (Ta=25 °C)

Parameter	Symbol	Condition	L2656			L2656-03			Unit
			Min.	Typ.	Max.	Min.	Typ.	Max.	
Peak emission wavelength	λp	I_F=50 mA	870	890	920	870	890	920	nm
Spectral half width	$\Delta\lambda$	I_F=50 mA	-	50	-	-	50	-	nm
Forward voltage	V_F	I_F=50 mA	-	1.45	1.6	-	1.45	1.6	V
Pulse forward voltage	V_{FP}	I_F=1 A	-	3.4	4.0	-	3.4	4.0	V
Reverse current	I_R	V_R=5 V	-	-	5	-	-	5	µA
Radiant flux	ϕe	I_F=50 mA	13	15	-	7.5	9	-	mW
Radiant illuminance	P_E	I_F=50 mA	-	1.7	-	-	4.4	-	mW/cm²
Rise time	tr	I_F=50 mA, 10 to 90 %	-	0.45	0.7	-	0.45	0.7	µs
Fall time	tf	I_F=50 mA, 90 to 10 %	-	0.45	0.7	-	0.45	0.7	µs

SOLID STATE DIVISION

HAMAMATSU

Infrared LED L2656 series

■ Emission spectrum

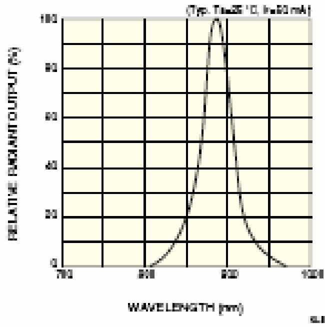

■ Radiant flux vs. forward current

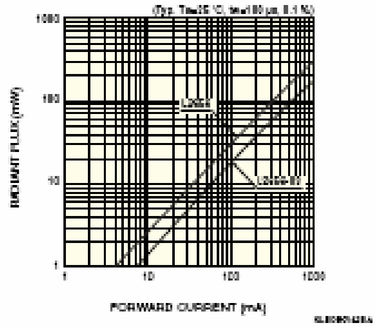

■ Forward current vs. forward voltage

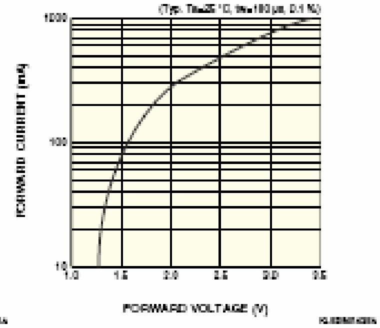

■ Directivity

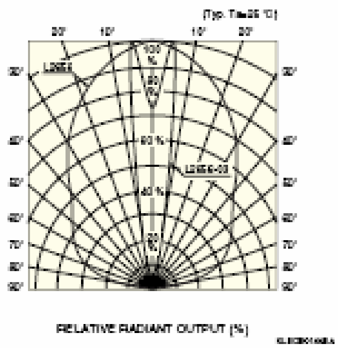

■ Radiant output vs. ambient temperature

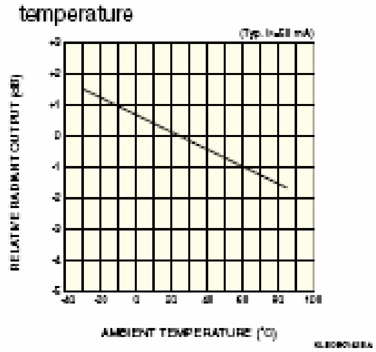

■ Allowable forward current vs. ambient temperature

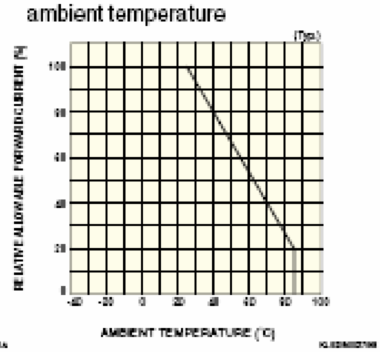

■ Allowable forward current vs. duty ratio

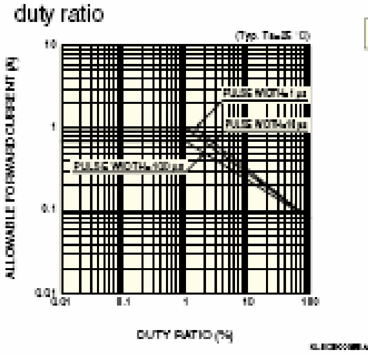

■ Dimensional outlines (unit: mm)

L2656

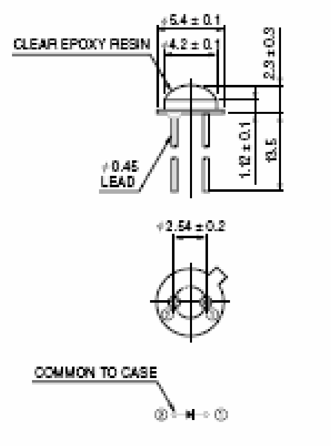

L2656-03

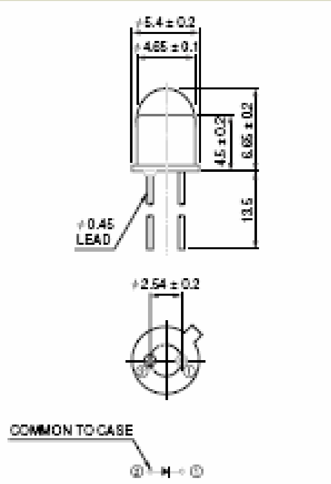

HAMAMATSU PHOTONICS K.K., Solid State Division
1126-1 Ichino-cho, Hamamatsu City, 435-8558 Japan, Telephone: (81) 053-434-3311, Fax: (81) 053-434-5184, http://www.hamamatsu.com
U.S.A.: Hamamatsu Corporation: 360 Foothill Road, P.O.Box 6910, Bridgewater, N.J. 08807-0910, U.S.A., Telephone: (1) 908-231-0960, Fax: (1) 908-231-1218
Germany: Hamamatsu Photonics Deutschland GmbH: Arzbergerstr. 10, D-82211 Herrsching am Ammersee, Germany, Telephone: (49) 08152-3750, Fax: (49) 08152-2658
France: Hamamatsu Photonics France S.A.R.L.: 8, Rue du Saule Trapu, Parc du Moulin de Massy, 91882 Massy Cedex, France, Telephone: 33-(1) 69 53 71 00, Fax: 33-(1) 69 53 71 10
United Kingdom: Hamamatsu Photonics UK Limited: 2 Howard Court, 10 Tewin Road, Welwyn Garden City, Hertfordshire AL7 1BW, United Kingdom, Telephone: (44) 1707-294888, Fax: (44) 1707-325777
North Europe: Hamamatsu Photonics Norden AB: Smidesvägen 12, SE-171 41 Solna, Sweden, Telephone: (46) 8-509-031-00, Fax: (46) 8-509-031-01
Italy: Hamamatsu Photonics Italia S.R.L.: Strada della Moia, 1/E, 20020 Arese, (Milano), Italy, Telephone: (39) 02-935-81-733, Fax: (39) 02-935-81-741

Cat. No. KLED1024E01
Apr. 2001 DN

PHOTODIODE

Si PIN photodiode
S3071, S3072, S3399, S3883

Large area, high-speed Si PIN photodiodes

S3071, S3072, S3399 and S3883 are Si PIN photodiodes having a relatively large active area from ϕ1.5 to ϕ6.0 mm yet they offer excellent frequency response from 40 to 300 MHz. These photodiodes are suitable for spatial light transmission and high-speed pulsed light detection.

Features

- Active area size
  S3071: ϕ5.0 mm
  S3072: ϕ3.0 mm
  S3399: ϕ3.0 mm
  S3883: ϕ1.5 mm
- Cut-off frequency
  S3071: 40 MHz (V_R=24 V)
  S3072: 45 MHz (V_R=24 V)
  S3399: 100 MHz (V_R=10 V)
  S3883: 300 MHz (V_R=20 V)
- High reliability: TO-5/8 metal package

Applications

- Spatial light transmission
- High-speed pulsed light detection

■ General ratings / Absolute maximum ratings

Type No.	Dimensional outline/ Window material *1	Package (mm)	Active area size (mm)	Effective active area (mm²)	Absolute maximum ratings: Reverse voltage VR Max. (V)	Power dissipation P (mW)	Operating temperature Topr (°C)	Storage temperature Tstg (°C)
S3071	①/K	TO-8	ϕ5.0	19.6	50	50	-40 to +100	-55 to +125
S3072	②/K	TO-5	ϕ3.0	7.0				
S3399	③/K		ϕ3.0	7.0	30			
S3883	④/K		ϕ1.5	1.7				

■ Electrical and optical characteristics (Typ. Ta=25 °C, unless otherwise noted)

Type No.	Spectral response range λ (nm)	Peak sensitivity wavelength λp (nm)	Photo sensitivity S (A/W): λp	660 nm	780 nm	830 nm	Short circuit current Isc 100 lx (μA)	Dark current ID (nA): Typ.	Max.	Temp. coefficient of ID TCID (times/°C)	Cut-off frequency fc RL=50 Ω (MHz)	Terminal capacitance Ct f=1 MHz (pF)	NEP (W/Hz^1/2)
S3071	320 to 1060	920	0.6	0.47	0.54	0.56	17	0.5 *3	10 *3	1.15	40 *3	18 *3	2.1×10^{-14} *3
S3072							6.5	0.3 *3	10 *3		45 *3	7 *3	1.7×10^{-14} *3
S3399	320 to 1000	840	0.6	0.45	0.58	0.6	5.6	0.1 *4	1.0 *4	1.12	100 *4	20 *4	9.4×10^{-15} *4
S3883							1.4	0.05 *2	1.0 *2		300 *2	6 *2	6.7×10^{-15} *2

*1: Window material K: borosilicate glass
*2: V_R=20 V
*3: V_R=24 V
*4: V_R=10 V

SOLID STATE DIVISION

HAMAMATSU

Si PIN photodiode S3071, S3072, S3399, S3883

■ Spectral response

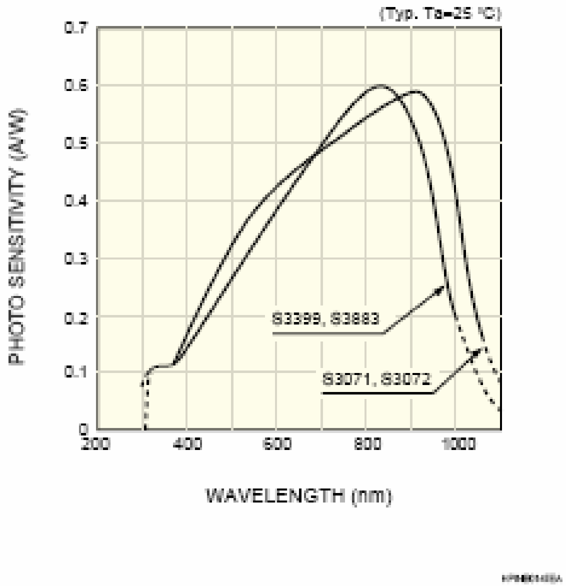

■ Photo sensitivity temperature characteristics

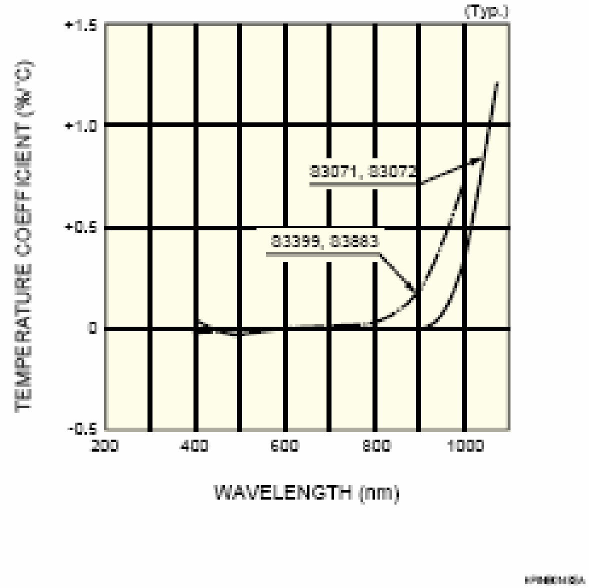

■ Dark current vs. reverse voltage

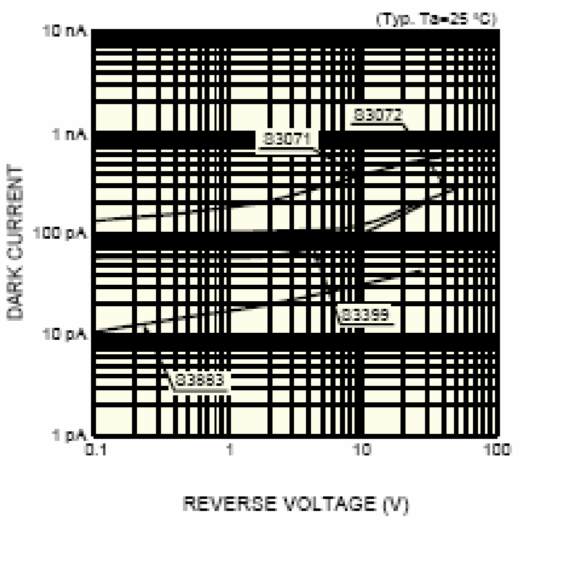

■ Terminal capacitance vs. reverse voltage

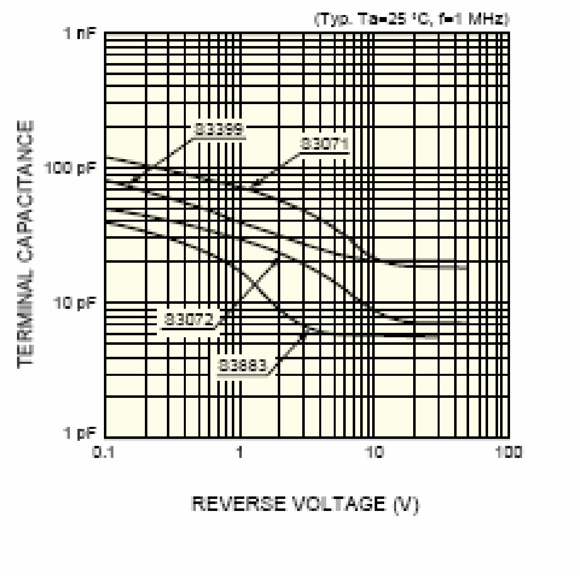

Si PIN photodiode S3071, S3072, S3399, S3883

■ Dimensional outline (unit: mm)

① S3071

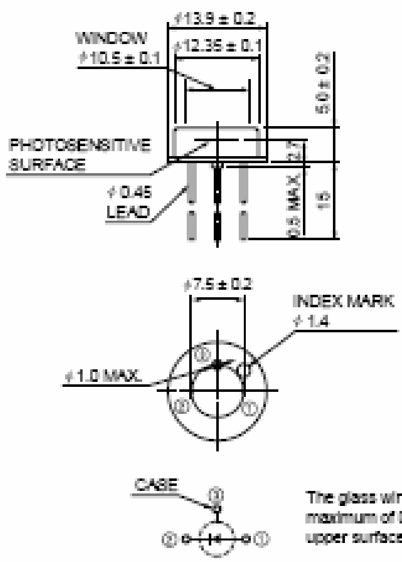

The glass window may extend a maximum of 0.3 mm above the upper surface of the cap.

② S3072

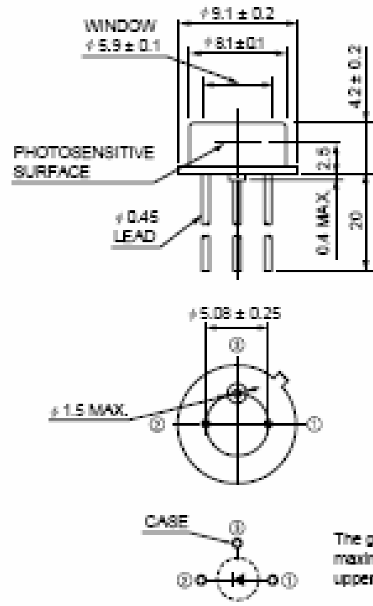

The glass window may extend a maximum of 0.2 mm above the upper surface of the cap.

③ S3399

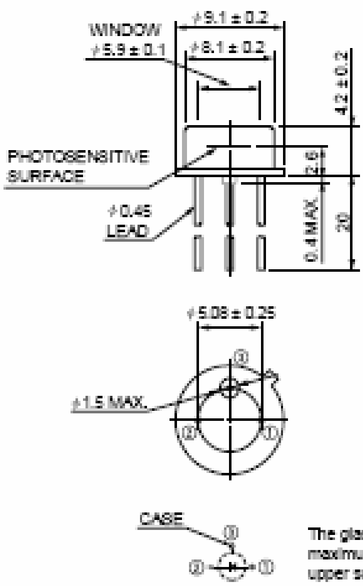

The glass window may extend a maximum of 0.2 mm above the upper surface of the cap.

④ S3883

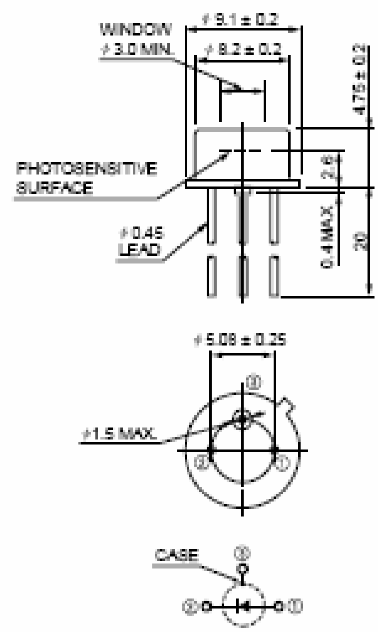

HAMAMATSU PHOTONICS K.K., Solid State Division
1126-1 Ichino-cho, Hamamatsu City, 435-8558 Japan, Telephone: (81) 053-434-3311, Fax: (81) 053-434-5184, http://www.hamamatsu.com
U.S.A.: Hamamatsu Corporation: 360 Foothill Road, P.O.Box 6910, Bridgewater, N.J. 08807-0910, U.S.A., Telephone: (1) 908-231-0960, Fax: (1) 908-231-1218
Germany: Hamamatsu Photonics Deutschland GmbH: Arzbergerstr. 10, D-82211 Herrsching am Ammersee, Germany, Telephone: (49) 08152-3750, Fax: (49) 08152-2658
France: Hamamatsu Photonics France S.A.R.L.: 8, Rue du Saule Trapu, Parc du Moulin de Massy, 91882 Massy Cedex, France, Telephone: 33-(1) 69 53 71 00, Fax: 33-(1) 69 53 71 10
United Kingdom: Hamamatsu Photonics UK Limited: 2 Howard Court, 10 Tewin Road, Welwyn Garden City, Hertfordshire AL7 1BW, United Kingdom, Telephone: (44) 1707-294888, Fax: (44) 1707-325777
North Europe: Hamamatsu Photonics Norden AB: Smidesvägen 12, SE-171 41 Solna, Sweden, Telephone: (46) 8-509-031-00, Fax: (46) 8-509-031-01
Italy: Hamamatsu Photonics Italia S.R.L.: Strada della Moia, 1/E, 20020 Arese, (Milano), Italy, Telephone: (39) 02-935-81-733, Fax: (39) 02-935-81-741

Cat. No. KPIN1044E02
Aug. 2004 DN

PHOTODIODE

Si photodiode
S2386 series

For visible to IR, general-purpose photometry

Features
- High sensitivity
- Low dark current
- High reliability
- High linearity

Applications
- Analytical equipment
- Optical measurement equipment

■ General ratings / Absolute maximum ratings

Type No.	Dimensional outline/ Window material *	Package (mm)	Active area size (mm)	Effective active area (mm^2)	Absolute maximum ratings: Reverse voltage V_R Max. (V)	Operating temperature Topr (°C)	Storage temperature Tstg (°C)
S2386-18K	①/K	TO-18	1.1 × 1.1	1.2	30	-40 to +100	-55 to +125
S2386-18L	②/L						
S2386-5K	③/K	TO-5	2.4 × 2.4	5.7			
S2386-44K			3.6 × 3.6	13			
S2386-45K			3.9 × 4.6	17.9			
S2386-8K	④/L	TO-8	5.8 × 5.8	33			

■ Electrical and optical characteristics (Typ. Ta=25 °C, unless otherwise noted)

Type No.	Spectral response range λ (nm)	Peak sensitivity wavelength λp (nm)	Photo sensitivity S (A/W): λp	GaP LED 560 nm	He-Ne laser 633 nm	GaAs LED 930 nm	Short circuit current Isc 100 lx Min. (μA)	Typ. (μA)	Dark current ID V_R=10 mV Max. (pA)	Temp. coefficient of ID TCID (times/°C)	Rise time tr V_R=0 V R_L=1 kΩ (μs)	Terminal capacitance Ct V_R=0 V f=10 kHz (pF)	Shunt resistance Rsh V_R=10 mV Min. (GΩ)	Typ. (GΩ)	NEP ($W/Hz^{1/2}$)
S2386-18K	320 to 1100	960	0.6	0.38	0.43	0.59	1	1.3	2	1.12	0.4	140	5	100	6.8×10^{-16}
S2386-18L							4	5.7							
S2386-5K							4.4	6.0	5		1.8	730	2	50	9.6×10^{-16}
S2386-44K							9.6	12	20		3.6	1600	0.5	25	1.4×10^{-15}
S2386-45K							12	17	30		5.5	2300	0.3		
S2386-8K							26	33	50		10	4300	0.2	10	2.1×10^{-15}

* Window material K: borosilicate glass, L: lens type borosilicate glass

SOLID STATE DIVISION

HAMAMATSU

■ Spectral response

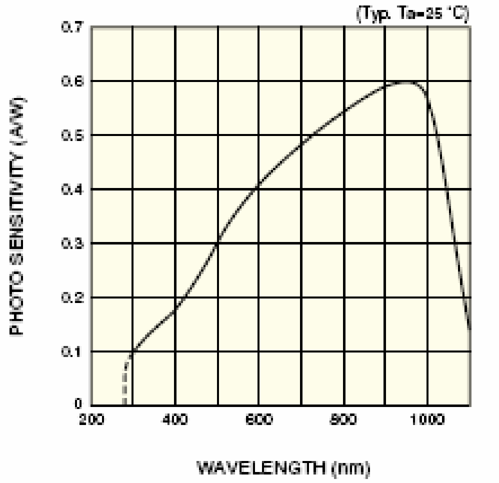

■ Photo sensitivity temperature characteristic

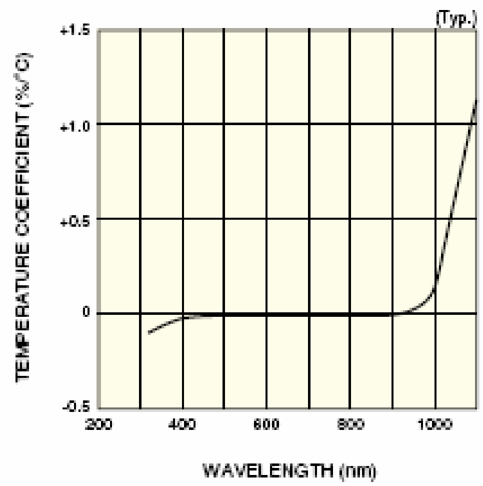

■ Directivity

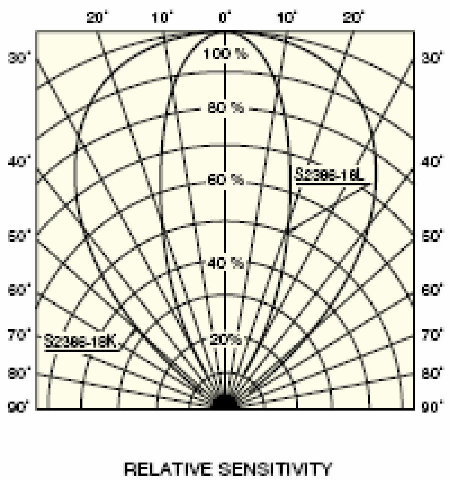

■ Rise time vs. load resistance

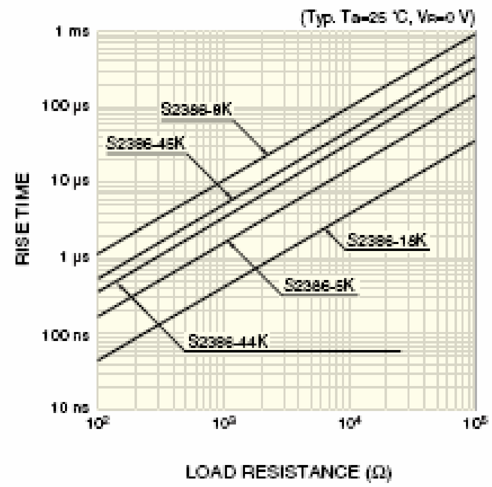

■ Dark current vs. reverse voltage

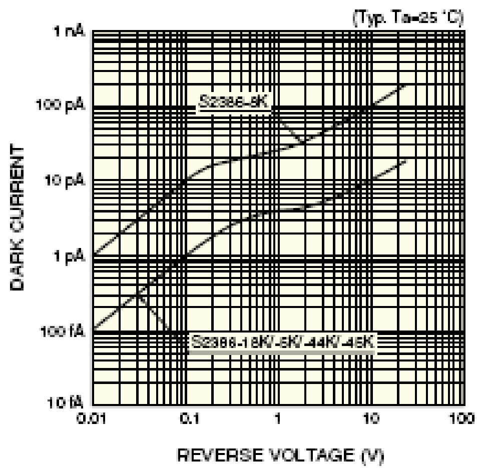

■ Shunt resistance vs. ambient temperature

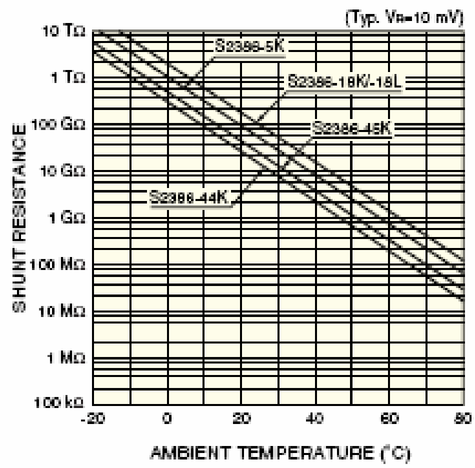

■ Dimensional outlines (unit: mm)

① S2386-18K

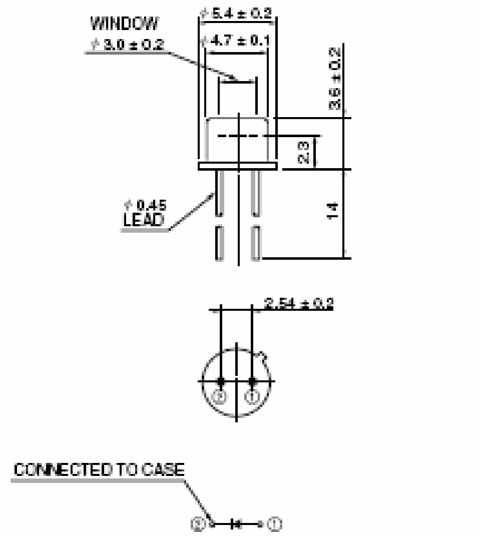

② S2386-18L

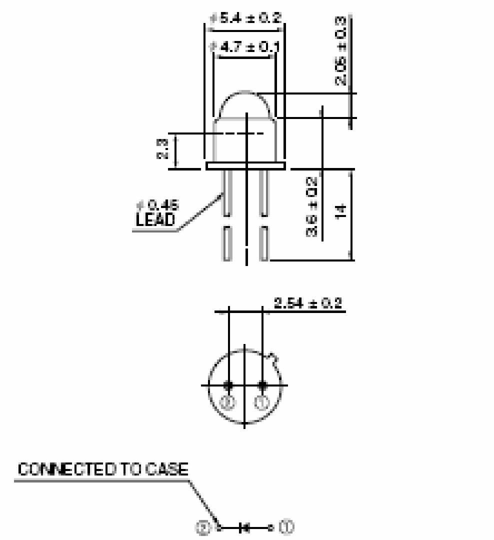

③ S2386-5K/-44K/-45K

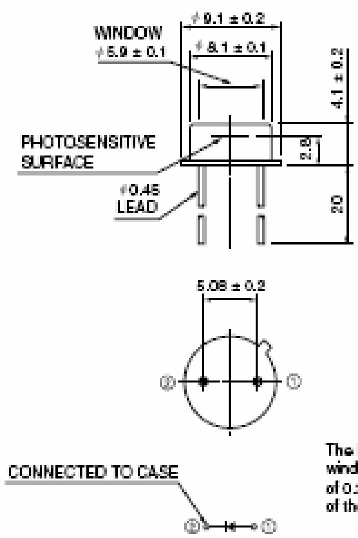

The K type borosilicate glass window may extend a maximum of 0.2 mm above the upper surface of the cap.

④ S2386-8K

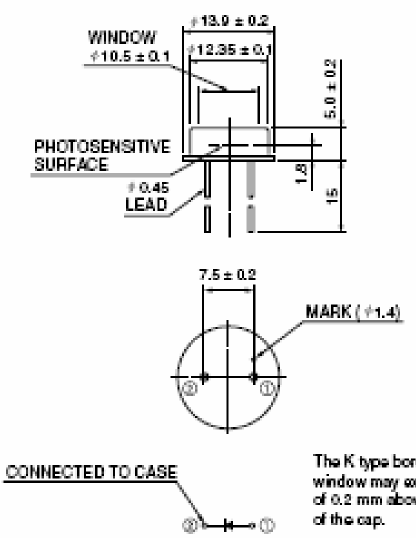

The K type borosilicate glass window may extend a maximum of 0.2 mm above the upper surface of the cap.

HAMAMATSU PHOTONICS K.K., Solid State Division
1126-1 Ichino-cho, Hamamatsu City, 435-8558 Japan, Telephone: (81) 053-434-3311, Fax: (81) 053-434-5184, http://www.hamamatsu.com
U.S.A.: Hamamatsu Corporation: 360 Foothill Road, P.O.Box 6910, Bridgewater, N.J. 08807-0910, U.S.A., Telephone: (1) 908-231-0960, Fax: (1) 908-231-1218
Germany: Hamamatsu Photonics Deutschland GmbH: Arzbergerstr. 10, D-82211 Herrsching am Ammersee, Germany, Telephone: (49) 08152-3750, Fax: (49) 08152-2658
France: Hamamatsu Photonics France S.A.R.L.: 8, Rue du Saule Trapu, Parc du Moulin de Massy, 91882 Massy Cedex, France, Telephone: 33-(1) 69 53 71 00, Fax: 33-(1) 69 53 71 10
United Kingdom: Hamamatsu Photonics UK Limited: 2 Howard Court, 10 Tewin Road, Welwyn Garden City, Hertfordshire AL7 1BW, United Kingdom, Telephone: (44) 1707-294888, Fax: (44) 1707-325777
North Europe: Hamamatsu Photonics Norden AB: Smidesvägen 12, SE-171 41 Solna, Sweden, Telephone: (46) 8-509-031-00, Fax: (46) 8-509-031-01
Italy: Hamamatsu Photonics Italia S.R.L.: Strada della Moia, 1/E, 20020 Arese, (Milano), Italy, Telephone: (39) 02-935-81-733, Fax: (39) 02-935-81-741

Cat. No. KSPD1035E02
Oct. 2002 DN